Algal Research 89 (2025) 104080

Contents lists available at ScienceDirect

Algal Research

journal homepage: www.elsevier.com/locate/algal

Unlocking biochemical profile of *Chaetoceros calcitrans*, *Cylindrotheca fusiformis*, and *Nannofrustulum shiloi* (Bacillariophyta) for nutritional and added-value applications

Ana S.P. Moreira [a,*,1], Helena R. Rocha [b,1], Susana Aveiro [c], Andreia S. Ferreira [d], Kayane Oliveira [d], Alexandra Conde [e], Marta Coelho [b], Alexandre M.C. Rodrigues [f], Natacha Coelho [f,g], Hugo Pereira [c], Ana Gomes [b], Manuela Pintado [b], Cláudia Nunes [h], Manuel A. Coimbra [d], Sónia P.M. Ventura [e], Rosário Domingues [a], Diana Lopes [a,*]

[a] *CESAM - Centre for Environmental and Marine Studies, Department of Chemistry, University of Aveiro, Campus Universitário de Santiago, 3810-193 Aveiro, Portugal*
[b] *CBQF—Centro de Biotecnologia e Química Fina—Laboratório Associado, Escola Superior de Biotecnologia, Universidade Católica Portuguesa, Rua Diogo Botelho, 1327, Porto 4169-005, Portugal*
[c] *GreenCoLab, Associação Oceano Verde, Universidade do Algarve, Campus de Gambelas, 8005-139 Faro, Portugal*
[d] *LAQV-REQUIMTE, Department of Chemistry, University of Aveiro, Campus Universitário de Santiago, 3810-193 Aveiro, Portugal*
[e] *CICECO - Aveiro Institute of Materials, Department of Chemistry, University of Aveiro, Campus Universitário de Santiago, 3810-193 Aveiro, Portugal*
[f] *Necton S.A., Belamandil, 8700-152 Olhão, Portugal*
[g] *MED (Instituto Mediterrâneo para a Agricultura, Ambiente e Desenvolvimento) & CHANGE – Global Change and Sustainability Institute, Faculdade de Ciências e Tecnologia, Campus de Gambelas, Universidade do Algarve, Ed. 8, 8005-139 Faro, Portugal*
[h] *CICECO – Aveiro Institute of Materials, Department of Materials and Ceramic Engineering, University of Aveiro, Campus Universitário de Santiago, 3810-193 Aveiro, Portugal*

ARTICLE INFO

Keywords:
Microalgae
Bacillariophytes
Lipidomics
Minerals
Sugars
Pigments
Amino acids

ABSTRACT

Diatoms have garnered attention as sources of natural bioactive compounds, making them attractive for developing high-value products for different biotechnological ends, particularly for nutritional applications. Despite their potential, the chemical composition of industrially produced biomass remains largely underexplored. In this context, this study was focused on a thorough characterisation of the biochemical profile of three marine diatom species produced outdoors in photobioreactors: *Chaetoceros calcitrans*, *Cylindrotheca fusiformis*, and *Nannofrustulum shiloi*. The proximal composition of biomasses accounted for 29–35 % ashes, 21–30 % proteins, 7–14 % lipids, 3–7 % carbohydrates, and 0.4–2 % pigments. Each species contained >35 % of essential amino acids, mainly alanine and leucine. Distinct soluble protein and peptide size distribution patterns were observed among the three species. Galactose (26–45 mol%), uronic acids (20–29 mol%), and glucose (3–21 mol %) were the main sugar residues found in all species. Galactose was mainly derived from floridoside and related compounds. The most abundant fatty acid was 20:5 *n*-3 in *C. calcitrans* (18 %), whereas in *C. fusiformis* was 16:1 *n*-7 (20 %) and 16:0 in *N. shiloi* (21 %). Lipidomics revealed 325 species of glycolipids, phospholipids, betaine lipids, sphingolipids, fatty amides, and sterol lipids, also with a distinct distribution along the lipid classes. *C. calcitrans* was the richest in chlorophylls (14 $mg.g^{-1}$) and carotenoids (8 $mg.g^{-1}$). In mineral analysis, calcium showed the highest difference, 66 $mg.g^{-1}$ in *N. shiloi*, 27 $mg.g^{-1}$ in *C. fusiformis*, and 4 $mg.g^{-1}$ in *C. calcitrans*. Overall, this study highlights the nutritional potential of industrially produced diatoms, with distinct chemical profile that can be explored for target applications.

* Corresponding authors.
E-mail addresses: ana.moreira@ua.pt (A.S.P. Moreira), dianasalzedaslopes@ua.pt (D. Lopes).
[1] These authors contributed equally to this work.

https://doi.org/10.1016/j.algal.2025.104080
Received 17 January 2025; Received in revised form 17 April 2025; Accepted 3 May 2025
Available online 5 May 2025

1. Introduction

Diatoms (Bacillariophyceae) are photosynthetic eukaryotic algae widely distributed in aquatic environments (marine and fresh water) and characterised by their unique silicified cell walls [1]. These organisms constitute a significant portion of the phytoplankton community, accounting for nearly half of marine primary production and playing a pivotal role in the biogeochemical cycling of nutrients and global carbon stabilisation by fixing a large part of ocean's CO_2 [2–4]. They represent the most diverse group of phytoplankton, comprising conservatively estimated one hundred thousand extant species [5]. Diatoms are widely known for their remarkable adaptability to environmental fluctuations and rapid growth rates [6,7], enabling their application in diverse biotechnology fields, such as bioremediation, aquaculture, and production of value-added metabolites [8].

In the last decades, diatoms have garnered attention as prolific producers of different added-value compounds, particularly pigments (such as carotenoids) and polyunsaturated fatty acids (PUFA) [9–12]. Diatoms contain different photoprotective carotenoids, including fucoxanthin and xanthophylls [13], which have found applications in food supplements, feed, and cosmetics [10,11]. Regarding lipids, diatoms are commonly rich in omega-3 PUFA, including eicosapentaenoic (EPA, 20:5*n*-3) and docosahexaenoic (DHA, 22:6*n*-3) acids, which have a recognised positive contribution to human and animal health [14,15]. Moreover, various groups of lipids, including polar lipids, steroids, oxylipins, and isoprenoids, have been reported in diatom species and associated with bioactive properties and health benefits [7]. However, despite their potential, the lipidomic characterisation of diatoms remains relatively underexplored.

Beyond pigments and lipids, diatoms produce a range of other valuable compounds, including polysaccharides and proteins [16]. The primary energy storage polysaccharide in diatoms is a β-1,3-glucan, known as chrysolaminaran, which has garnered interest due to its crucial role in nutrition and its functions as an antioxidant, immunoregulatory, anticoagulant, and anti-inflammatory agent [17]. Like other photoautotrophs, diatoms synthesise a wide range of amino acids for building proteins and producing other biologically active compounds, such as polyamines, glutathione, and heme [18–20]. These organisms are also recognised for their high protein quality, as their amino acid composition indicates excellent nutritional value [21,22]. For example, the essential amino acid index of the diatom *Phaeodactylum tricornutum* is comparable to that of an ideally balanced protein, such as egg albumin [22]. Despite their potential, diatoms remain underexplored as sources of bioactive peptides for functional foods and ingredients. Studies on marine diatom stains, like *Bellerochae* and *Nitzschia*, have shown that their protein hydrolysates exhibit promising antioxidant and antihypertensive properties [23,24].

Among hundreds of diatom species, understanding the biochemical composition of diatoms, particularly of industrially produced biomass, is essential to unlocking their full potential across various sectors. Therefore, investigating their biochemical composition and capacity to produce biologically active compounds is crucial for uncovering their potential biotechnological applications. This strategic approach aligns with the goals of the Blue Growth strategy—an initiative by the European Commission that aims to foster sustainable growth in the marine sector [25].

In this study, the biomass of three marine diatom species – *Chaetoceros calcitrans* (*C. calcitrans*), *Cylindrotheca fusiformis* (*C. fusiformis*), and *Nannofrustulum shiloi* (*N. shiloi*) – grown in outdoor photobioreactors were selected for a broad biochemical characterisation. Accordingly, a thorough analysis of proximal composition and the profile of pigments, fatty acids, lipids, sugars, amino acids, peptides, and minerals was conducted. By revealing the detailed chemical profiles of these diatoms, this research seeks to unravel their potential for nutritional applications and enhance their value.

2. Material and methods

2.1. Production of biomass

The microalgae biomass of *Chaetoceros calcitrans, Cylindrotheca fusiformis*, and *Nannofrustulum shiloi* was supplied by Necton S.A. (Portugal). Cultures from all strains were individually scaled from the laboratory up to closed 3 m^3 Flat Panel photobioreactors in the exterior, during the summer season. Throughout the production period, a water spray system was used to cool the photobioreactors when their temperature reached 33 °C. Even so, the cultures temperature ranged between 18 and 35 °C, 12 to 36 °C, and 16 to 34 °C for *C. calcitrans*, *C. fusiformis* and *N. shiloi*, respectively. Maximum sun irradiance during production was on average 1844, 1778, and 1747 μmol m^{-2} s^{-1}, around 14 h, for *C. calcitrans*, *C. fusiformis* and *N. shiloi*, respectively. Cultures were kept monoalgal and NutriBloom Plus® was used as culture medium, with a nitrate concentration of 4 mM, and silica supplementation of 440 mM. Salinity was 35 ppt and maximum pH was set at 8.5 for the three cultures, with automatic CO_2 injecton on demand. Following cultivation, cultures were harvested via centrifugation at a controlled speed to obtain a wet paste that was packed and frozen at −20 °C. The frozen paste was freeze-dried, milled and vacuum-packed for subsequent analysis. Dry weight (DW) biomass refers to the weight of freeze-dried biomass.

2.2. Determination of moisture and ash content

The freeze-dried biomass of *C. calcitrans*, *C. fusiformis*, and *N. shiloi* (50 mg, in triplicate) was dried at 105 °C for 15 h in ceramic crucibles. After cooling to room temperature in a desiccator, the crucibles were weighed to determine moisture content by gravimetry. For ash determination, the same biomass (previously dried at 105 °C) was incinerated in a muffle furnace at 575 °C for 6 h, then cooled to room temperature and weighed [26].

2.3. Elemental analysis and protein estimation

Elemental analysis (C, H, N, and S) was conducted using spray-dried biomass (2 mg, in triplicate) on a Leco Truspec-Micro CHNS 630–200-200 elemental analyser, with a combustion furnace temperature of 1075 °C and an afterburner temperature of 850 °C. Nitrogen was detected via thermal conductivity. Protein content was estimated from total nitrogen using a nitrogen-to-protein conversion factor of 4.78 [27].

2.4. Pigment analysis

The extraction of chlorophylls and carotenoids was done using conventional organic solvents, 99 % (*v*/v) ethanol, and the dry biomass of the three diatoms under study. The extraction conditions were the same for the three diatoms, with a Solid Liquid Ratio (SLR) of 0.05 g biomass.mL^{-1} solvent, at constant temperature (25 °C) and stirring for 30 min in an orbital rotor (80 rpm). After the extraction, the samples were centrifuged for 15 min at 15,000 rpm, from which the supernatant was recovered and used for analysis. The solvent was added to the recovered pellet, and the extraction process was repeated until the recovered supernatant was colourless. The absorbance spectra of the various extracts were determined between 230 and 700 nm on a UV–Vis microplate reader (SpectraMax, USA). The chlorophylls and carotenoids were estimated using chlorophyll *a* and fucoxanthin's standard from Sigma-Aldrich, with purity ≥85 % and ≥ 95 %, respectively, as they are the most abundantly present in diatoms [28]. Chlorophyll *a* was quantified according to the calibration curve previously drawn at 662 nm on the same equipment. Fucoxanthin was further quantified using a reverse phase-high performance liquid Chromatography (RP-HPLC) analysis, where a calibration curve was previously established for 450 nm, and an optimised detection method was used [29]. The separation of the

compounds was carried out with a gradient elution program at a flow rate of 1 mL·min^{-1}, at 30 °C, using a Kinetex® C18 column (250 × 4.6 nm; 5 μm, Phenomenex). The method was adapted from previous studies, with an injection volume of 30 μL, and a mobile phase consisting of water (B) and acetonitrile: methanol (70:30) (C), both previously degassed and filtered. The solvent gradient was 15 % of solvent A (ultrapure water with 0.1 % of formic acid) and 85 % of solvent C for 2 min, followed by an increase of up to 100 % for 5 min, and maintaining that condition for 5 min, returning to 15 % of B and 85 % of C during 3 min and equilibrating for 2 min. All the quantification tests were carried out in triplicate.

2.5. Lipids analysis

2.5.1. Lipids extraction

Lipids were extracted from 25 mg of freeze-dried biomass of *C. calcitrans*, *C. fusiformis*, and *N. shiloi* using a modified Folch's method [30]. Biomass was mixed with 2 mL of dichloromethane (DCM):methanol (MeOH) (2:1, *v*/v) in a glass tube and vortexed for 2 min, followed by 30 min of incubation on ice using an orbital shaker. Afterwards, the mixture underwent centrifugation at 2000 rpm for 10 min, and the organic phase was collected. This process was repeated three times. The organic phase was then completely dried under a nitrogen stream. To eliminate non-lipid compounds, the dried extract was dissolved in 3 mL of DCM:MeOH (2:1, *v*/v) and 0.75 mL of Milli-Q water were added. The mixture was vortexed for 2 min and then centrifuged at 2000 rpm for 10 min to induce phase separation. The organic phase was collected, and the aqueous phase was re-extracted by adding 2 mL of DCM, followed by vortexing for 1 min and centrifugation for 5 min at 2000 rpm (this step was repeated two more times). The combined organic phases were then filtered into a new glass tube using a paper filter (WhatmanTM) to remove suspended particles and dried under a nitrogen stream. The resulting lipid extracts were transferred to pre-weighed amber vials, dried under nitrogen, weighed, and stored at −20 °C until further analysis. The total lipid content was then determined gravimetrically and expressed as a percentage of DW biomass.

2.5.2. Fatty acids profiling by GC–MS

The fatty acid methyl esters (FAME) were prepared by alkaline transesterification of *C. calcitrans*, *C. fusiformis*, and *N. shiloi* lipid extracts. The dried lipid extracts were combined with 1 mL of an internal standard solution (1.0 μg.mL^{-1} of methyl nonadecanoate in *n*-hexane), followed by the addition of 200 μL of KOH solution (2.0 M in MeOH), and vortexed for 2 min. Subsequently, 2 mL of saturated NaCl solution (10 mg.mL^{-1} in water) was added, and the mixture was centrifuged at 2000 rpm for 5 min. The upper organic phase (600 μL) was transferred to a new glass tube and dried under a stream of nitrogen. For GC–MS analysis, the dried FAME were dissolved in 100 μL of 99 % *n*-hexane, and 2 μL of this solution was injected into a GC–MS equipped with a DB-FFAP column (30 m of length, 0.32 mm of internal diameter and 0.25 μm of film thickness, J&W Scientific, Folsom, CA, USA). The oven temperature was programmed to start at 58 °C (held for 2 min), followed by a linear increase to 160 °C at a rate of 25 °C min^{-1}, then a linear increase of 2 °C min^{-1} to 210 °C, and finally a 20 °C min^{-1} increase until reaching 225 °C (held for 15 min). The GC–MS system was coupled with an Agilent 5973 Network Mass Selective Detector (Agilent Technologies), operating in electron impact mode at 70 eV and scanning *m/z* range of 50–550 in a 1-s cycle in full-scan mode acquisition. The injector and detector temperatures were set at 220 °C and 230 °C, respectively. Helium gas was used as the carrier at a flow rate of 1.4 mL min^{-1}. The data acquisition software was GCMS5977B/Enhanced MassHunter. The acquired data were analysed using the software Agilent MassHunter Qualitative Analysis 10.0. FAME were identified by comparing their retention times and mass spectra with those of FAME standards (C6–C24, Supelco 37 Component FAME Mix). Further confirmation was achieved considering the mass spectra of the "Lipid Web" and the NIST Library.

2.5.3. Total lipidome profiling by C18 LC-MS/MS

The total lipid extracts were analysed by reverse-phase liquid chromatography coupled to high-resolution tandem mass spectrometry (C18-LCMS/MS) using an Ultimate 3000 Dionex (Thermo Fisher Scientific, Bremen, Germany) equipped with an Ascentis® Express 90 Å C18 column (Sigma-Aldrich®, 2.1 × 100 mm, 2.7 μm) coupled to a Q-Exactive® hybrid quadrupole Orbitrap mass spectrometer (Thermo Fisher Scientific, Bremen, Germany). For this analysis, the total lipid extracts were resuspended in dichloromethane to achieve a concentration of 1 μg μL^{-1}. A volume of 5 μL of a mixture containing 20 μL of lipid extract, 72 μL of a solvent system of isopropanol:methanol (1:1, *v*/v), and 8 μL of a mixture of phospholipid standards (1,2-dimyristoyl-*sn*-glycero-3-phosphocholine - 0.04 μg, N-heptadecanoyl-D-erythro-sphingosylphosphorylcholine - 0.04 μg, 1,2-dimyristoyl-*sn*-glycero-3-phosphoethanolamine - 0.04 μg, 1-nonadecanoyl-2-hydroxy-*sn*-glycero-3phosphocholine - 0.04 μg, 1,2-dipalmitoyl-*sn*-glycero-3-phosphoinositol - 0.08 μg, 1′,3′-bis[1,2-dimyristoyl-*sn*-glycero-3-phospho]-glycerol - 0.16 μg; 1,2-dimyristoyl-*sn*-glycero-3-phosphoglycerol - 0.024 μg, N-heptadecanoyl-D-erythro-sphingosine - 0.08 μg, 1,2-dimyristoyl-*sn*-glycero-3-phospho-L-serine −0.08 μg; 1,2-dimyristoyl-*sn*-glycero-3-phosphate - 0.16 μg) was injected, for each sample, into the column at 50 °C and at a flow rate of 260 μL min^{-1}. Mobile phase A consisted of Milli-Q water/acetonitrile (ACN) (40/60 %) with 10 mM ammonium formate and 0.1 % formic acid, while mobile phase B comprised isopropanol/ACN (90/10 %) with 10 mM ammonium formate and 0.1 % formic acid. The elution started with 32 % of mobile phase B, followed by the following gradient: 45 % B (1.5 min), 52 % B (4 min), 58 % B (5 min), 66 % B (8 min), 70 % B (11 min), 85 % B (14 min), 97 % B (18 min), 97 % B (25 min), 32 % B (25.01 min, followed by an 8-min re-equilibration period before the next injection). The mass spectrometer operated simultaneously in positive mode (electrospray voltage 3.0 kV) and negative mode (electrospray voltage 2.7 kV). The gas flow was 35 U, the auxiliary gas was 3 U, the capillary temperature was 320 °C, the S-lenses RF was 50 U, and the probe temperature was 300 °C. Data acquisition was performed in full scan mode with a high resolution of 70,000 and automatic gain control (AGC) target of 3 × 10^6, in an *m/z* range of 200–1600, with 2 micro scans, and a maximum injection time (IT) of 100 ms. Tandem mass spectra (MS/MS) were obtained with a resolution of 17,500, AGC target of 1 × 10^5, 1 micro scan, and a maximum IT of 100 ms. The cycles consisted of a full-scan mass spectrum and 10 data-dependent MS/MS scans, repeated continuously throughout the experiments with a dynamic exclusion of 30 s and an intensity threshold of 8 × 10^4. The normalised collision energy (CE) ranged between 20, 24, and 28 eV in the negative mode and 25 and 30 eV in the positive mode. Data was acquired using the Xcalibur data system (V3.3, Thermo Fisher 6 Scientific, Bremen, Germany).

The identification of lipid species was achieved using the raw files acquired in MS/MS mode and converted by the ABF converter against the lipid database provided by MS-DIAL 4 software. Tolerances for MS and MS/MS search were set at 0.01 Da and 0.05 Da, respectively. The identified and approved lipid species areas were integrated with MZmine 3.9.0 software. The peak area of each lipid species was normalised against the peak area of the lipid standard with the closest retention time. Venn diagram representation was performed using an open-source tool (https://www.interactivenn.net/).

2.6. Sugar analysis

Neutral sugars were determined as alditol acetates as described by Ferreira et al. [31]. Briefly, a pre-hydrolysis of the sample (2 mg) was performed with 72 % (*w*/w) sulfuric acid for 3 h at room temperature with occasional stirring, followed by a hydrolysis with 1 M sulfuric acid for 2.5 h at 100 °C. A 2-deoxyglucose was added as an internal standard. Monosaccharides were reduced with sodium borohydride and

acetylated with acetic anhydride, using methyl-imidazole as a catalyst. The resulting alditol acetate derivatives were analysed by gas chromatography coupled with a flame ionisation detector (GC-FID, Perkin Elmer Clarus 400, USA), following the chromatographic conditions described by Lopes et al. [32]. The alditol acetates were also injected in a GC-qMS (Shimadzu GC–MS QP2010) equipped with a ZB-5HT INFERNO capillary column (J&W Scientific, Folsom, CA, USA), with 30 m length, 0.25 mm of internal diameter, and 0.25 μm of film thickness to identify and quantify the naturally methylated sugar residues and the amino sugar residues, such as glucosamine. The samples were injected in "split" mode with the injector temperature at 250 °C. The following oven temperature programme was used: an initial temperature of 140 °C; an increase of 5 °C·min^{-1} until 180 °C and held for 1 min; an increase of 10 °C·min^{-1} until 280 °C. The carrier gas has helium with a flow of 32.1 mL·min^{-1}. Uronic acids (UA) were quantified using the *m*-phenylphenol colourimetric method, using a calibration curve with D-galacturonic acid (10–100 μg·mL^{-1}) [31].

To identify and quantify floridoside, the different diatoms were analysed after reduction and acetylation using 2-deoxyglucose (1.0 mg·mL^{-1}) as internal standards. The alditol acetates were dissolved in anhydrous acetone and analysed by GC-qMS (Shimadzu GC–MS QP2010) equipped with a ZB-5HT INFERNO capillary column (J&W Scientific, Folsom, CA, USA), with 30 m length, 0.25 mm of internal diameter, and 0.25 μm of film thickness. The samples were injected in "split" mode with the injector temperature at 340 °C. The temperature program used was as follows: an initial temperature of 140 °C; an increase of 5 °C·min^{-1} until 250 °C (held for 5 min); an increase of 5 °C·min^{-1} until 300 °C (held for 1 min). The carrier gas has helium with a flow of 8.1 mL·min^{-1}. Floridoside was quantified using a calibration curve (r^2 = 0.9979). L- and D-isofloridoside and digalactosylaglycerol were identified by the retention time and by comparing the standard mass spectrum and quantified as floridoside equivalents.

2.7. Amino acid analysis

Microalgae samples were subjected to acid hydrolysis to determine the total amino acid content. Approximately 100 mg of each microalgae sample was weighed into small SPME vials, to which 2 mL of 6 M HCl (Sigma-Aldrich, Inc., St. Louis, USA) were added. The mixture was vortexed to ensure proper mixing. A needle was inserted into the vial septum for oxygen release, while another needle connected to a nitrogen stream was introduced. Nitrogen gas was bubbled through the sample for 1 min, after which the oxygen outlet needle was removed, and nitrogen bubbling continued for an additional 3 min. The nitrogen inlet needle was removed, and the vial was tightly sealed with tape around the cap and sides. The sealed vials were placed in an oven at 115 °C for 20 h to complete the hydrolysis process. Following hydrolysis, the vials were allowed to cool to room temperature. The hydrolysed samples were diluted with 5 mL of ultra-pure water, and the pH was adjusted to 3.5 using 10 M NaOH. The solution was then transferred to a 10 mL volumetric flask, diluted to the mark with ultra-pure water, and the final solution was filtered through a 0.22 μm filter.

A liquid chromatograph equipped with a high-resolution fluorescence detector and "autosampler" was used to detect and quantify the total amino acids. The chromatographic separation was performed on a Chromolith® Performance RP18e column (100–4.6 mm) by Sigma Aldrich (REF: 1.02129.0001). Eluents were degassed using an ultrasonic bath. The elution program included: i) flow rate starting at 0.9 mL min^{-1} and increasing to 1.2 mL min^{-1} at specific intervals and ii) gradient: starting with 10 % eluent B, ramping up to 100 % eluent B, then returning to the initial conditions. The complete program lasted 55 min, including stabilisation phases. Fluorescence detection parameters were set with an excitation wavelength of 356 nm and an emission wavelength of 445 nm, with a sensitivity factor of 1. The data collection rate was 2 Hz, and the lamp mode was set to "Standard." The chromatographic column temperature was maintained at 25 °C throughout the analysis.

For HPLC analysis, two eluents were prepared: a) eluent A: 2.8 g of Na_2HPO_4, 7.6 g of $Na_2B_4O_7{\cdot}10H_2O$, and 0.06 g of NaN_3 (Sigma-Aldrich, Inc., St. Louis, USA) were dissolved in ultra-pure water, and the pH was adjusted to 8.2 with HCl, making up a total volume of 2 L; b) eluent B: a mixture of 450 mL of methanol, 450 mL of acetonitrile (Fisher Chemical, USA), and 100 mL of ultra-pure water was prepared to a total volume of 1 L. Several solutions and reagents were prepared as follows to ensure proper derivatisation of amino acids, allowing their detection and quantification through HPLC with fluorescence detection: c) borate buffer (pH 9.5): for 1 L, 6.2 g of H_3BO_3 was dissolved in ultra-pure water, the pH was adjusted to 9.5 with 4 M NaOH, and the solution was diluted to 1 L; d) internal standard (IS) solution: homoserine (0.01 g) (Sigma-Aldrich, USA) was dissolved in 50 mL of 0.1 M HCl to prepare a stock solution of 200 mg L^{-1}. This was then diluted tenfold with 0.1 M HCl to obtain a 20 mg L^{-1} working solution; e) Reagent A: 3 mL of the IS solution (20 mg L^{-1}) was mixed with 100 μL of mercaptoethanol (Fluka Analytical, USA) and 0.5 g of sodium tetraphenylborate (Merck, Germany), then diluted to 25 mL with borate buffer. This solution was stored cold and used within one week; f) reagent B: 0.6 g of iodoacetic acid (Sigma-Aldrich, USA) was dissolved in 15 mL of borate buffer, adjusted to pH 9.5 with 4 M NaOH, and diluted to 20 mL with borate buffer; g) reagent C: 0.175 g of *o*-Phthalaldehyde (OPA) (Sigma-Aldrich, USA) was dissolved in 5 mL of methanol, followed by the addition of 0.5 mL of mercaptoethanol. The solution was diluted to 25 mL with borate buffer, and nitrogen gas was bubbled through it. The solution was stored in the cold and covered with aluminium foil to protect it from light. A calibration curve was prepared using a 100 mg L^{-1} amino acid stock solution in 0.1 M HCl. Standard solutions with concentrations ranging from 1 to 30 mg L^{-1} were prepared by diluting the stock solution in 0.1 M HCl.

2.8. Size exclusion chromatography for determination of the peptide and protein profile

The microalgae samples (freeze-dried biomass) were reconstituted to a concentration of 50 mg mL^{-1} in ultrapure water. The reconstituted samples were centrifuged at 14500 rpm for 5 min. The supernatant was filtered through a 0.22 μm filter and then analysed by gel filtration chromatography. The column was operated at a flow rate of 0.5 mL min^{-1} using a phosphate buffer (0.025 M, pH 7) supplemented with NaCl (0.15 M) and NaN3 (0.02 % *w/v*). A calibration curve was prepared using protein standards with known molecular weights, including Thyroglobulin (669 kDa), Ferritin (440 kDa), Aldolase (158 kDa), Conalbumin (75 kDa), Ovalbumin (43 kDa), Carbonic anhydrase (29 kDa), Ribonuclease A (13.7 kDa), and Aprotinin (6.5 kDa). The setup consisted of an AKTA pure 25 L system from GE Healthcare Life Sciences (Freiburg, Germany), featuring two pumps with pressure control for column protection. A gel filtration column prepacked with Superdex® 200 10/300 GL was connected in series with a Superdex Peptide 10/300 GL column (both from GE Healthcare Life Sciences, Freiburg, Germany). Sample analysis was conducted using a U9-L UV multiwavelength detection monitor set at 280 nm, and data were processed with UNICORN 7.0 software [33].

2.9. Mineral analysis

The microwave digestion method used for this analysis was based on the CEM MARS 6 Microwave Acid Digestion Method Note Compendium for plant tissue [34]. First, 0.5 g of each microalgae sample was accurately weighed and placed into a digestion vessel. To this, 10 mL of concentrated nitric acid was added, and the mixture was gently swirled and left to settle for approximately 15 min before closing the vessel. The digestion process used the MARS ONE system. The heating program involved ramping the temperature to 200 °C over 15 min, holding it at 200 °C for an additional 15 min, maintaining a pressure of 800 psi, and

applying power in the 900–1800 W range without stirring.

2.10. Statistical analysis

Univariate statistical analyses on the data of proximal composition were performed using GraphPad Prism 9 software. Normality was tested using Shapiro−Wilk test, corroborating a normal distribution. Significant differences between the groups were then evaluated using two-way ANOVA with Tukey's post hoc test, considering differences significant at $p < 0.05$.

3. Results and discussion

3.1. Composition of the biomass

The biomass of *C. calcitrans*, *C. fusiformis*, and *N. shiloi* was analysed for moisture, ash, lipids, proteins, and sugars content, with data expressed as a percentage of dry weight (DW, freeze-dried) biomass (Table 1). *C. calcitrans* and *C. fusiformis* displayed similar content of ash (29.25 ± 0.04 %; 29.09 ± 0.12 %), whereas *N. shiloi* stood out for the higher ash (34.64 ± 0.64 %) and lower lipid (7.00 ± 0.44 %) contents. These differences may be related to the cellular structures of these species. Diatoms are characterised by their silica-based cell walls [35], and the higher ash content in *N. shiloi* could indicate a thicker silica wall. This may result in lower lipid extraction yield, as the thicker silica barrier could hinder the ability of solvents to access the cell membranes.

C. calcitrans exhibited a lower carbohydrate content (3.16 ± 0.11 %) and higher protein content (30.14 ± 0.16 %) than the other diatom species. These differences in the chemical composition highlight the potential for selecting specific species for targeted applications. For example, the ash content, representing the total mineral composition, makes diatom species with higher levels (*C. calcitrans* and *C. fusiformis*) ideal for mineral supplementation in animal feeds and other nutritional products. Likewise, diatom species with higher protein content (*C. calcitrans*) could be favoured for protein-rich applications.

Although the presented values reflect the composition of these diatoms, it is well-known that their biochemical profiles are modulated by the growth conditions, which can be explored to enhance their qualities and composition in target compounds. For instance, lipid accumulation in diatoms can be significantly improved by applying physiological stresses such as nutrient limitation, extreme temperatures, or varying light intensities [36–38]. Also, ash content and other components are influenced by the growth conditions. For example, higher ash content (45.4–50.5 %) and lowest protein content (15.3–16.9 %), were previously reported for *C. calcitrans* cultivated with control and optimised culture media [39], compared to the data obtained in this study. Thus, it is important to emphasise that the compositional data and the detailed results presented in the following sections should be considered as general guidance for these three species and interpreted in the context of the cultivation conditions described in Section 2.1 of the methodology.

Table 1
Composition of ***C. calcitrans, C. fusiformis***, and *N. shiloi* biomass, expressed as percentage (%) of dry weight (DW, freeze-dried) biomass. Values are the mean ± standard deviation (SD) of three replicates (***n*** = 3).
Significant differences between the groups were revealed using two-way ANOVA with Tukey's post hoc test. Values in the same row followed by the same letter are not significantly different at $p < 0.05$.

	C. calcitrans	*C. fusiformis*	*N. shiloi*
Moisture	7.56 ± 0.26^{a}	7.66 ± 0.12^{a}	6.99 ± 1.22^{a}
Ash	29.25 ± 0.04^{a}	29.00 ± 0.12^{a}	34.64 ± 0.64^{b}
Lipids	12.40 ± 1.14^{a}	14.27 ± 0.12^{b}	7.00 ± 0.44^{c}
Proteins *	30.14 ± 0.16^{a}	24.30 ± 0.47^{b}	21.11 ± 0.25^{c}
Sugars #	3.16 ± 0.11^{a}	6.01 ± 0.42^{b}	7.07 ± 0.34^{c}

* Calculated as N of elemental analysis x 4.78; # Total sugars determined by the sum of neutral sugars analysis and uronic acids content.

Considering that the three diatoms analysed in this study were cultivated during the summer season under similar environmental conditions - specifically with respect to temperature, salinity, and irradiance - the differences observed in their composition are more possible related to species-specific characteristics rather than to variations in culture conditions.

3.2. Pigments

The total content of chlorophylls and carotenoids is shown in Table 2. As supported by the literature, chlorophyll *a* and fucoxanthin are the most abundant chlorophyll and carotenoid present in diatoms, respectively [28]. Among the three diatoms analysed in this study, the chlorophyll content ranged from 2.90 to 14.16 mg·g DW biomass $^{-1}$, while the carotenoid content ranged from 0.98 to 7.51 mg·g DW biomass $^{-1}$ (Table 2). The lowest content of chlorophylls and carotenoids was identified in *N. shiloi*, but the values obtained are about 3-fold higher than those previously reported [28]. Such differences may be related to differences in the growth conditions of the microalgae, as previously demonstrated in literature [40]. Considering the highest content of chlorophylls and carotenoids found in *C. calcitrans*, this diatom can be more attractive than *C. fusiformis* and *N. shiloi* for applications related to the valorisation of natural pigments. In particular, fucoxanthin (the predominant carotenoid in diatoms) has interesting applications as food additives, in medicine [41], and as pharmaceutic and cosmetic ingredients [42].

3.3. Fatty acids profile

The profile of total esterified fatty acids of *C. calcitrans*, *C. fusiformis*, and *N. shiloi* (Table 3) revealed a prevalence of C16 and C20 fatty acids across the three diatom species. The five most abundant fatty acids identified in the three diatoms included saturated fatty acid (SFA) 16:0, monounsaturated fatty acid (MUFA) 16:1 *n*-7, and polyunsaturated fatty acid (PUFA) 16:3 *n*-4. However, certain PUFA were particularly noteworthy for their higher content in specific diatoms, such as 20:5 *n*-3 in *C. calcitrans*, 20:4 *n*-6 in *C. fusiformis*, and 16:4 *n*-1 in *N. shiloi*. Also, SFA 14:0 was among the five most abundant fatty acids of *C. calcitrans* and *C. fusiformis*. Despite some variations, the fatty acids identified as most abundant are in line with what was previously reported for *C. calcitrans* [39,43] and *C. fusiformis* [44].

The overall fatty acids' content in *N. shiloi* (3.32 ± 0.24 mg·g DW biomass^{-1}) was much lower compared to the data obtained for *C. calcitrans* (14.25 ± 0.81) and *C. fusiformis* (19.72 ± 2.43), although PUFA were more abundant than SFA and MUFA across all three species. However, the distribution of PUFA between *n*-3 and *n*-6 differed: *C. calcitrans* had the highest *n*-3 content, *C. fusiformis* had the highest *n*-6 content, and *N. shiloi* exhibited equal amounts of *n*-3 and *n*-6. This results in a variation in the *n*-6/*n*-3 ratio, with *C. calcitrans* being the only species where this ratio was <1 (considered favourable for health benefits).

Various evidence indicated that *n*-3 fatty acids significantly benefit animal and human health by reducing inflammation, decreasing fat accumulation in various organs, and supporting the proper functioning of cells and tissues [16]. Research has also shown that a lower *n*-6/*n*-3

Table 2
Estimated content of chlorophylls and carotenoids (mg·g DW biomass $^{-1}$) in ***C. calcitrans***. ***C. fusiformis***, and *N. shiloi* diatoms. The values represent the mean ± standard deviation (SD) of three replicates (***n*** = 3).

	C. calcitrans	*C. fusiformis*	*N. shiloi*
Chlorophylls (mg·g DW biomass $^{-1}$)	14.16 ± 0.41	12.18 ± 0.18	3.289 ± 0.03
Carotenoids (mg·g DW biomass $^{-1}$)	7.51 ± 0.25	2.90 ± 0.08	0.98 ± 0.02

Table 3
Fatty acid composition (mg·g DW biomass^{-1}) of ***C. calcitrans***, ***C. fusiformis***, and *N. shiloi* diatoms determined by gas chromatography–mass spectrometry (GC–MS). Values are the mean ± standard deviation (SD) of five replicates (***n*** = 5).

Fatty acids	*C. calcitrans*	*C. fusiformis*	*N. shiloi*
14:0	1.85 ± 0.11	2.11 ± 0.28	0.15 ± 0.02
15:0	0.16 ± 0.01	t	t
16:0	1.81 ± 0.12	3.68 ± 0.40	0.70 ± 0.06
16:1 *n*-7	1.31 ± 0.07	3.90 ± 0.50	0.52 ± 0.05
16:1 *n*-5	0.06 ± 0.01	0.21 ± 0.03	t
16:1 *n*-9	0.13 ± 0.01	t	t
16:2 *n*-6	0.25 ± 0.02	0.15 ± 0.02	t
16:2 *n*-4	0.80 ± 0.05	1.09 ± 0.15	0.08 ± 0.01
16:3 *n*-4	2.45 ± 0.14	3.09 ± 0.39	0.32 ± 0.03
16:4 *n*-1	0.76 ± 0.06	0.30 ± 0.05	0.44 ± 0.03
18:0	0.66 ± 0.28	0.32 ± 0.08	0.13 ± 0.06
18:1 *n*-9	0.13 ± 0.01	0.63 ± 0.09	t
18:1 *n*-7	0.21 ± 0.01	0.20 ± 0.03	0.06 ± 0.01
18:2 *n*-6	0.12 ± 0.01	0.33 ± 0.05	0.10 ± 0.01
18:3 *n*-6	0.40 ± 0.03	0.22 ± 0.04	0.13 ± 0.01
18:4 *n*-3	0.19 ± 0.01	t	0.13 ± 0.01
20:4 *n*-6	0.32 ± 0.02	2.07 ± 0.29	0.16 ± 0.02
20:5 *n*-3	2.63 ± 0.17	1.31 ± 0.17	0.29 ± 0.03
∑ FA	14.25 ± 0.81	19.72 ± 2.43	3.32 ± 0.24
∑ SFA	4.48 ± 0.41	6.15 ± 0.61	0.99 ± 0.08
∑ MUFA	1.84 ± 0.10	4.97 ± 0.65	0.66 ± 0.06
∑ PUFA	7.92 ± 0.50	8.60 ± 1.17	1.67 ± 0.15
∑ *n*-3 PUFA	2.83 ± 0.19	1.36 ± 0.18	0.42 ± 0.04
∑ *n*-6 PUFA	1.09 ± 0.07	2.76 ± 0.40	0.41 ± 0.04
n-6/*n*-3 ratio	0.39 ± 0.01	2.04 ± 0.03	0.97 ± 0.01

Abbreviations: MUFA, monounsaturated fatty acids; PUFA, polyunsaturated fatty acids; SFA, saturated fatty acids; t, traces (<0.1 mg g^{-1} DW biomass).

ratio is associated with a reduced risk of coronary heart disease, as *n*-6 PUFA are considered less beneficial due to their pro-inflammatory properties compared to *n*-3 PUFA (REF). Both eicosapentaenoic acid (EPA, 20:5 *n*-3) and docosahexaenoic acid (DHA, 22:6 *n*-3), along with other PUFA, are key nutritional components in the tissues of many fish, crustaceans, and molluscs [45]. For this reason, EPA and DHA have been successfully incorporated into aquaculture feeds for both adult and larval stages, improving larval growth rates and enhancing the reproductive potential of marine organisms. Given their numerous health benefits, PUFA — particularly *n*-3 PUFA such as EPA and DHA— are essential as supplements for food and feed, creating an urgent demand for affordable and sustainable biological sources of these important compounds. Among the three diatom species under study, *C. calcitrans* stands out for its higher content in EPA (20:5*n*-3).

3.4. Lipid profile

The lipidome of *C. calcitrans*, *C. fusiformis*, and *N. shiloi* was characterised by C18-LC-MS, allowing the identification at the lipid species level and the determination of fatty acid composition for most cases. In total, 325 lipid species were identified and distributed across different lipid classes (Supplementary Table S1). These included various classes of glycolipids, namely monogalactosyldiacylglycerol (MGDG), monogalactosylmonoacylglycerol (MGMG), digalactosyldiacylglycerol (DGDG), digalactosylmonoacylglycerol (DGMG), and sulfoquinovosyldiacylglycerol (SQDG). Phospholipid classes identified in the diatom lipidome included phosphatidylcholine (PC), lysophosphatidylcholine (LPC), phosphatidylethanolamine (PE), lysophosphatidylethanolamine (LPE), phosphatidylinositol (PI), phosphatidylglycerol (PG), and lysophosphatidylglycerol (LPG). Also, other classes of phospholipids that are not common in algae were identified, including bismonoacylglycerolphosphate (BMP) and hemibismonoacylglycerophosphate (HBMP) (as classified in MS-DIAL) [46]. BMP are also named as monoacylglycerophosphomonoradylglycerols (in LIPIDMAPS) [47]. Additionally, several classes of betaine lipids were detected in the diatom lipidome, including diacylglyceryltrimethylhomoserine (DGTS), monoacylglyceryltrimethylhomoserine (MGTS), diacylglycerylcarboxyhydroxymethylcholine (DGCC), and monoacylglycerylcarboxyhydroxymethylcholine (MGCC). The identified sphingolipid classes included ceramide (Cer) and hexosylceramide (HexCer), as well as other classes of sphingolipids less reported in algae, ceramide phosphoethanolamines (PE-Cer) and sulfonolipid (SL). Additionally, less common classes of fatty amides, such as N-acyl glycine (NAGly), N-acyl glycyl serine (NAGlySer) and N-acyl ornithine (NAOrn) were detected. Ubiquinones, also known as coenzyme Q (CoQ), were also present, including CoQ8, CoQ9, and CoQ10. The neutral glycerolipids identified in the diatom lipidome included diacylglycerols (DG), and triacylglycerols (TG).

The identification of the lipids species of the different lipid classes was supported by the interpretation of the MS/MS fragmentation, which was previously well described for typical lipid classes found in microalgae [26]. Notably, several uncommon classes were identified herein for diatoms, which are not usually identified in other microalgae, and thus, the MS/MS spectra are shown in Supplementary material (Figs. S1-S7). These uncommon lipid classes included BMP, HBMP, PE-Cer, SL, NAGly, NAGlySer, and CoQ9. Interestingly, sulfonolipids (SL) were previously reported in a marine diatom, *Nitzschia alba* [48]. Sulfonolipids are also reported as an unusual class of bacterial lipids [49], and thus, their relationship with the microbiome cannot be excluded. Head group-acylated lipids have been found in algae and plants [50]. Although not reported in algae, HBMP species were previously found in oat seeds but named acylphosphatidylglycerol (acyl-PG) [51]. Ubiquinones were already reported in algae, namely the occurrence of CoQ10 was reported for *Isochrysis galbana* [52]. CoQ10 is widely used in cosmetic formulations for skin's defence against oxidative stress and to reduce skin ageing [53].

When comparing the lipidome of three diatoms, it was observed that, out a total of 325 lipid species identified in this study (Supplementary Table S1), 268 were present in all the diatoms (Fig. 1). In addition, few lipid species were found exclusively in each diatom: 4 in *C. calcitrans*, 1 in *C. fusiformis*, and 1 in *N. shiloi*. Also, some lipid species were found only in two of the three studied diatoms: 25 in *C. calcitrans* and *C. fusiformis*; 16 in *C. fusiformis* and *N. shiloi*; and 10 in *C. calcitrans* and *N. shiloi*.

The distribution of lipid species along the glycolipid classes of MGDG, DGDG and SQDG (Fig. 2), the phospholipid classes of PC, PE, PI,

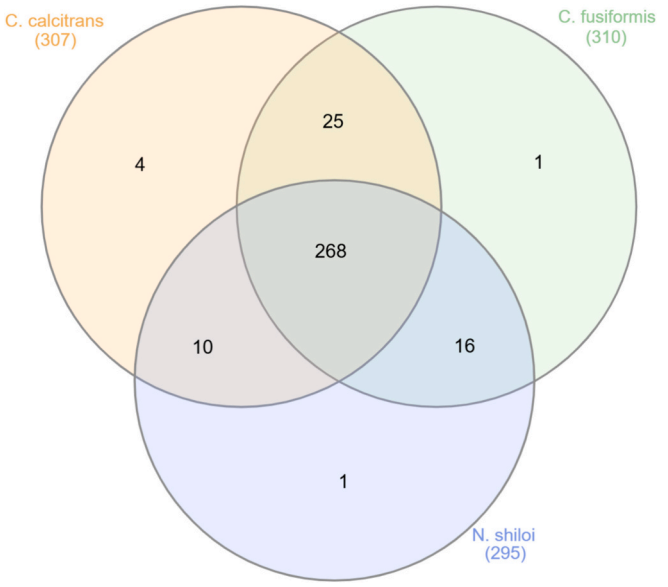

Fig. 1. Venn diagram representing the number of unique and common lipid species in the diatoms *C. calcitrans*, *C. fusiformis*, and *N. shiloi*.

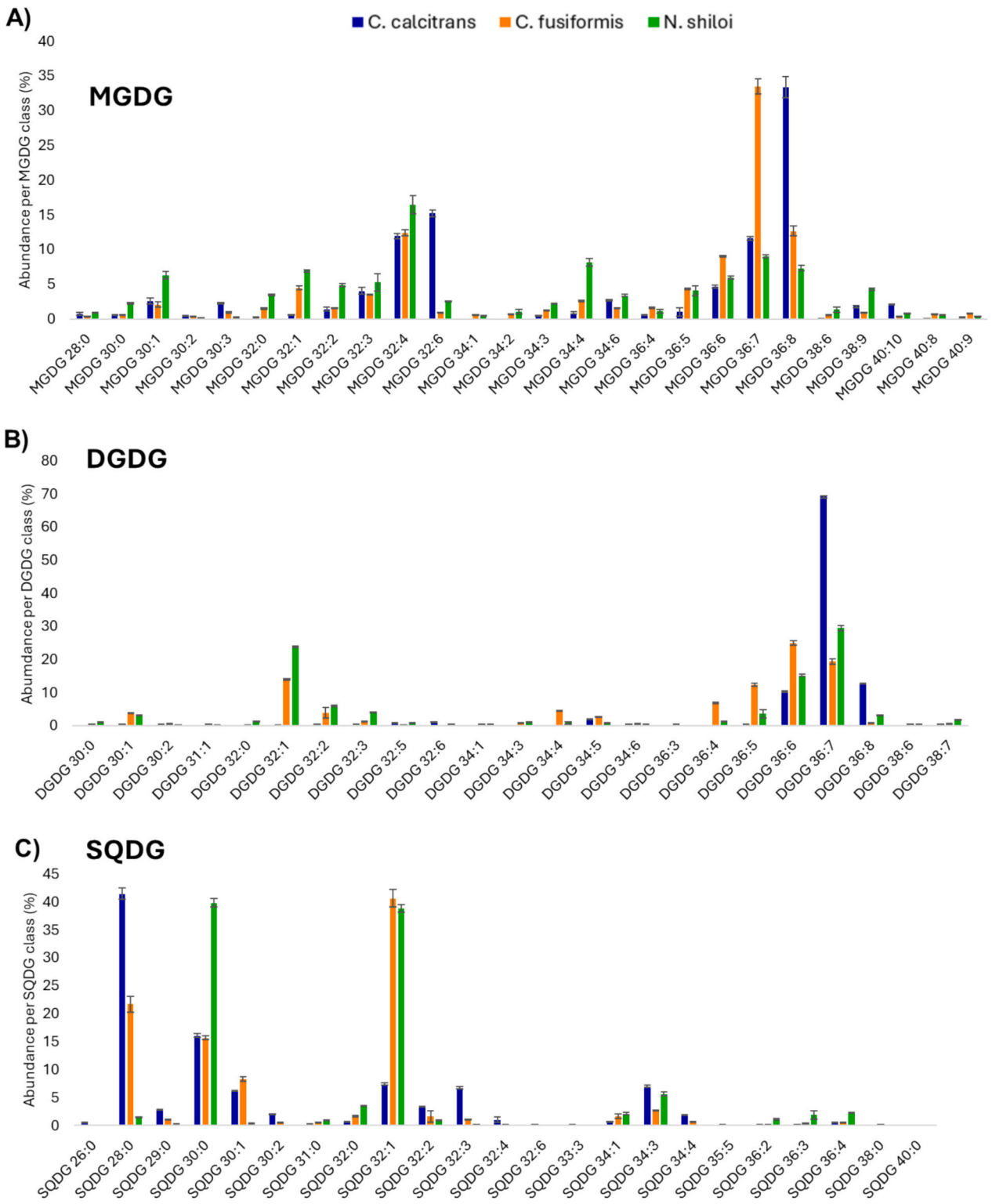

Fig. 2. Distribution of the diacyl lipid species identified in *C. calcitrans*, *C. fusiformis*, and *N. shiloi* across the glycolipid classes: A) monogalactosyldiacylglycerol (MGDG), B) digalactosyldiacylglycerol (DGDG), C) sulfoquinovosyldiacylglycerol (SQDG).

and PG (Fig. 3) and betaine lipid classes of DGTS and DGCC (Fig. 4) are also shown. The distribution of lipid species along the lyso lipid classes (LPC, LPE, LPG, DGMG, MGMG, MGTS, and MGCC) and the neutral lipids (DG and TG) can be consulted in Supplementary Figs. S8-S12. The distribution of the abundance of the lipid species by lipid class is different for each microalga, highlighting the specificity of the lipidome of each diatom species. Indeed, it is following previous work that mapped the lipid composition and profile of microalgae, suggesting a species-specific lipidome [54].

In the MGDG class, the most abundant lipid species were distinct among three diatoms (MGDG 36:8 in *C. calcitrans*, MGDG 36:7 in *C. fusiformis* and MGDG 32:4 in *N. shiloi*). The three species contained one fatty acid in common (16:3). The DGDG class is also dominated by highly unsaturated species, primarily consisting of 36-carbon chains.

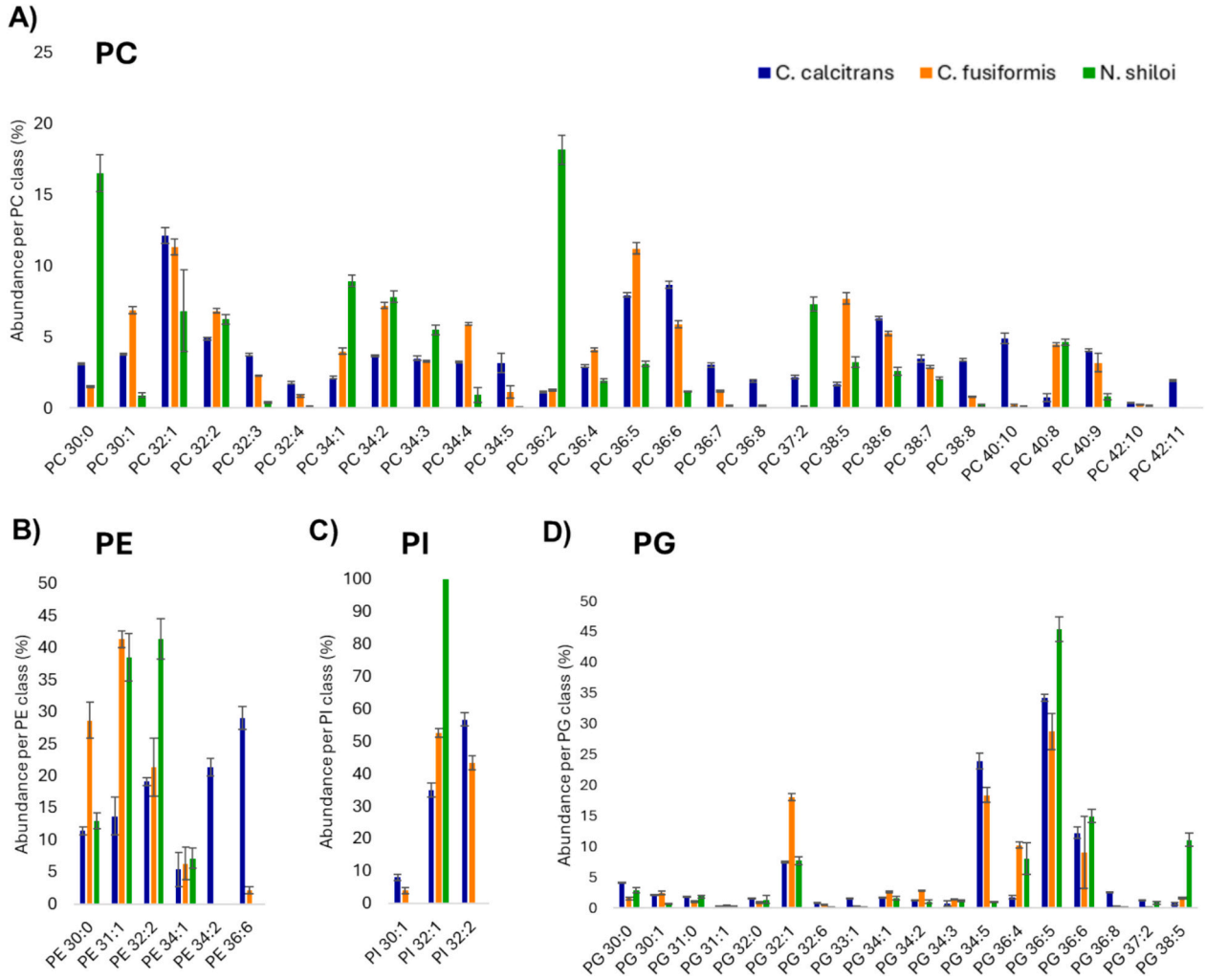

Fig. 3. Distribution of the diacyl lipid species identified in *C. calcitrans*, *C. fusiformis*, and *N. shiloi* across phospholipid classes: A) phosphatidylcholine (PC), B) phosphatidylethanolamine (PE), C) phosphatidylinositol (PI), and D) phosphatidylglycerol (PG).

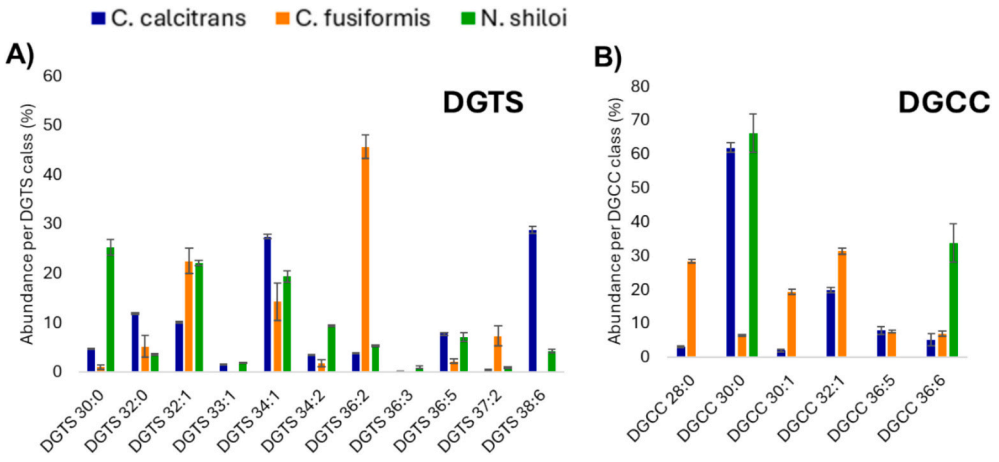

Fig. 4. Distribution of the diacyl lipid species identified in *C. calcitrans*, *C. fusiformis*, and *N. shiloi* across betaine lipid classes: A) diacylglyceryltrimethylhomoserine (DGTS) and B) diacylglycerylcarboxy-hydroxymethylcholine (DGCC).

DGDG 36:7, corresponding to DGDG 16:2_20:5, was the most abundant lipid species in *C. calcitrans* and *N. shiloi*, while DGDG 36:6, corresponding to DGDG 16:2_20:4, was the most abundant in *C. fusiformis*. The most abundant lipid species in the SQDG class were predominantly saturated and monounsaturated. SQDG 28:0 (14:0/14:0) and SQDG 32:1 (14:0_16:1) were the most predominant in *C. calcitrans* and *C. fusiformis*, respectively. Both SQDG 30:0 (14:0_16:0) and SQDG 32:1 (14:0_16:1) were abundant in *N. shiloi*.

Regarding the phospholipids (Fig. 3), the PC profile of *N. shiloi* differed from the other two diatoms, with the most abundant PC species containing 0 to 2 double bonds (e.g., PC 30:0, PC 34:1, PC 36:2). In contrast, except for PC 32:1, which is the most abundant mono-unsaturated PC species in both *C. calcitrans* and *C. fusiformis*, PC species with higher degrees of unsaturation were more prevalent in *C. calcitrans* (e.g., PC 36:5, PC 36:6) and *C. fusiformis* (e.g., PC 36:5, PC 38:5).

In the PE class, the most abundant lipid species in *C. calcitrans* were PE 36:6 and 34:2, whereas lipid species with lower carbon chains (C30 to C32) were the most abundant in *C. fusiformis* (PE 31:1 and PE 30:0) and *N. shiloi* (PE 32:2 and PE 31:1). In the PI class, PI 32:1 was the only lipid species identified in *N. shiloi*. In the PG class, PG 36:5 was the most abundant species in all three diatoms, corresponding to C16/C20 forms (16:1_20:4 and 16:0_20:5). Additionally, PG 34:5 (16:3_18:2) showed high abundance in both *C. calcitrans* and *C. fusiformis*. Also, PG 32:1 (16:0_16:1 and 14:0_18:1) was more abundant in *C. fusiformis* than in other diatoms.

Regarding betaine lipids (Fig. 4), DGTS 36:2 (18:1/18:1) was the predominant lipid species in *C. fusiformis*, with other species being the most abundant in *C. calcitrans* (DGTS 38:6 and DGTS 34:1) and *N. shiloi* (DGTS 30:0, DGTS 32:1 and DGTS 34:1). Also, DGCC 30:0 was the predominant lipid species in *C. calcitrans* and *N. shiloi*, but not in *C. fusiformis*.

In the TG class (Supplementary Table S1), *C. calcitrans* was characterised by the most abundant species having 1 and 6 double bonds, while the most prevalent species in *C. fusiformis* had 1 and 2 double bonds. In *N. shiloi*, the most abundant species had 0, 1 and 3 double bonds.

Few studies have explored the lipid characterisation of these diatom species, limiting direct comparisons with the current study. However, a study investigating the lipidome of *Cylindrotheca closterium* under nitrogen starvation identified several species of SQDG, MGDG, DGDG, and TG [55]. Remarkably, all MGDG, DGDG, and SQDG species reported in that study were also identified in *C. fusiformis* in the present research. In terms of TG species, nearly all identified in the previous study were found here as well, with only four exceptions: TG 50:5, TG 56:10, TG 56:9, and TG 56:8 [55]. One of the most abundant species in all three diatoms was TG 48:1, corresponding to TG 16:0_16:0_16:1 (Supplementary Table S1). This TG species has also been reported as one of the most abundant TG in *Cylindrotheca closterium* [55]. Betaine lipids containing a carboxyhydroxymethylcholine group (DGCC and MGCC) are less commonly reported in algae than those containing a trimethylhomoserine group (DGTS and MGTS). Indeed, DGCC and MGCC have been reported as characteristic of the phylum Haptophyta [26,56].

Of note, polar lipids have garnered increasing interest for added value apllications. In fact, some of the polar lipid species from algae have been associated with bioactive properties, namely anti-inflammatory glycolipids (e.g. DGDG 34:5 and MGDG 36:5), phospholipids (e.g. PC 40:10) and betaine lipids (e.g. DGTS 36:5) [57], also identified in this study. Beyond their bioactive properties, polar lipids hold immense potential in various industrial applications, including food, pharmaceutical and cosmetics.

In the food sector, polar lipids are commonly used as natural food emulsifier in processing and stabilisation aids in manufacturing food products like chocolates and baked goods [58]. Recent evidence suggests that synthetic emulsifiers may contribute to obesity-related metabolic disorders and inflammatory bowel disease (IBD), raising concerns about their safety. Lecithins, a mixture of phospholipids and other polar lipids, particularly those of marine origin, present a natural-based alternative to synthetic emulsifiers [59]. Rich in omega-3 PUFA, marine lecithins improve product stability and offer health benefits, acting as preventive and protective agents against inflammatory disorders. Moreover, polar lipids from marine sources provide essential fatty acids and choline, making them valuable for functional food formulations and dietary supplements to improve overall nutrition and health.

In the pharmaceutical industry, polar lipids play a critical role in advanced drug delivery systems. Phospholipids are used to create bilayer vesicles known as liposomes, which enhance the delivery of drugs by improving their solubility, stability, and bioavailability. Lipid-based drug delivery systems have emerged as a promising technology for addressing the challenges of poorly water-soluble drugs. Encapsulating or solubilising drugs in lipid-based excipients improves absorption and enhances therapeutic efficacy. This technology has found applications in delivering a wide range of pharmaceuticals, making polar lipids indispensable in modern drug delivery strategies [60].

In cosmetics, polar lipids derived from algae have emerged as active, natural, safe, and biomimetic ingredients, appealing to consumers increasingly concerned about the potential toxicity of synthetic ingredients. These lipids act as multifunctional components, offering both functional and therapeutic benefits. They serve as effective moisturisers by forming protective barriers on the skin to prevent water loss and enhance hydration. Additionally, they possess physiological properties such as anti-ageing effects, inhibiting matrix metalloproteinases and promoting skin hydration [61]. Their stabilising properties ensure consistent texture and integrity in creams and lotions, while their bioactive compounds reduce inflammation and support skin repair [57].

3.5. Carbohydrates profile

Despite their different content of total carbohydrates (Table 1), the three diatoms were mainly composed of galactose (26–45 mol%), uronic acids (20–29 mol%), and glucose (3–21 mol%), with minor amounts of mannose, xylose, ribose, fucose, and rhamnose. Moreover, glucosamine and the naturally methylated sugar 3-methylgalactose were also detected in the three diatoms, while 3-methylfucose and 3-methylmannose were only observed for *C. fusiformis* (Table 4).

Considering that all the quantified glucose residues are originated from hydrolysis of intracellular β-1,3-glucan, which is a glucose polysaccharide present in diatoms [62], the variation of glucose suggest that

Table 4
Carbohydrate's composition of ***C. calcitrans***, ***C. fusiformis***, and *N. shiloi* diatoms. Values are the mean ± standard deviation (SD) of three replicates (***n*** = 3).

Carbohydrates (mol%)	*C. calcitrans*	*C. fusiformis*	*N. shiloi*
Rha	2.06 ± 0.15	4.62 ± 0.68	1.44 ± 0.14
Fuc	3.61 ± 0.37	0.83 ± 0.21	t
3-MeFuc	nd	t	nd
Rib	11.19 ± 0.45	4.39 ± 0.39	2.89 ± 0.29
Ara	0.65 ± 0.21	nd	t
Xyl	9.61 ± 0.64	8.12 ± 0.62	5.56 ± 0.32
Man	5.23 ± 0.54	11.06 ± 1.65	5.93 ± 0.28
3-MeMan	nd	t	nd
Gal	45.04 ± 2.39	26.01 ± 0.50	33.66 ± 1.06
3-MeGal	t	t	t
Glc	3.13 ± 1.02	16.11 ± 0.42	20.90 ± 0.64
GlcN	t	t	t
UA	19.47 ± 0.57	28.87 ± 1.71	29.13 ± 1.15
Chrysolaminaran (mg·g^{-1} DW)	**1.01 ± 0.31**	**9.71 ± 0.58**	**14.68 ± 1.02**
Floridoside (mg·g^{-1} DW))	**6.44 ± 0.58**	**4.44 ± 1.32**	**18.35 ± 0.95**
Isofloridoside (D and L) / floridoside eq g^{-1} DW)	**0.51 ± 0.12**	**0.92 ± 0.35**	**8.64 ± 0.74**
Digalactosylaglycerol (floridoside eq g^{-1} DW)	**1.95 ± 0.33**	**1.03 ± 0.13**	**3.13 ± 0.22**

Abbreviations: Rha, ramnose; Fuc, fucose; 3-MeFuc, 3-*O*-methylfucose; Rib, ribose; Ara, arabinose; Xyl, xylose; Man, mannose; 3-MeMan, 3-*O*-methylmannose; Gal, galactose; 3-MeGal = 3-*O*-methylgalactose; Glc, glucose; GlcN, glucosamine; UA, uronic acids; t, trace (< 0.5 mol%); nd, not detected.

the β-1,3-glucan content varied between the analysed diatom species. The highest content in β-1,3-glucan was observed *in N. shiloi* (14.7 mg.g^{-1} DW biomass), followed by *C. fusiformis* (9.7 mg.g^{-1} DW biomass), with the lowest in *C. calcitrans* (1.0 mg.g^{-1} DW biomass). The content of total carbohydrates, and more specifically of β-glucan, may vary within microalgae species, and on the growth conditions, namely growth rates [63] and nutrients availability [64]. Specifically, Reitan et al. [63] observed a variation in the total carbohydrate content in response to changes in relative growth rate, with the extent of this variation differing among the microalgae species. The carbohydrate content of *C. calcitrans* did not vary significantly with the growth rate, whereas other diatom species (*Chaetoceros muelleri*) yielded significantly increased content with reduced growth rate [63]. Granum and Myklestad [64] investigated the effects of NH_4^+ assimilation on β-1,3-glucan metabolism in the N-limited marine diatom *Skeletonema costatum*. At the onset of dark NH_4^+ assimilation, biosynthesis of amino acids coincided with a significant decrease in cellular glucan (28 % within 3 h), suggesting that glucan is the ultimate substrate for β-carboxylation and amino acid biosynthesis in the dark [64]. Also, different growth conditions can explain the fact that glucose (and not galactose as in this work) was the main monosaccharide identified in *N. shiloi* isolated from the Adriatic Sea [28].Galactose residues were also one of the most representative sugar residues identified in the three analysed diatoms (26–45 mol%). A part of the galactose is a component of glycolipids identified by LC-MS (section 3.3). To evaluate if the galactose residues also derived from floridoside (2-α-O-D-galactopyranosyl glycerol) and isofloridoside (1-α-O-g alactopyranosylglycerol), these glycerol galactosides were determined for the three species of marine diatoms, although these compounds are usually associated with red algae [65].

N. shiloi presented the highest content in floridoside (18.4 mg.g^{-1} DW), followed by *C. calcitrans* and *C. fusiformis* (6.4 and 4.4 mg.g^{-1} DW, respectively). *N. shiloi* also revealed the highest amount of D- and L-isofloridoside (8.6 mg floridoside eq.g^{-1} DW), in comparison with the two other diatoms (0.5–0.9 mg floridoside eq g^{-1} DW). In addition, digalactosylaglycerol was also identified as being more abundant in *N. shiloi* (3.1 mg floridoside eq.g^{-1} DW) when compared with *C. calcitrans* and *C. fusiformis* (1.0 and 1.9 mg floridoside eq.g^{-1} DW, respectively). These results showed that 41 %, 27 %, and 88 % of the galactose residues of *C. calcitrans*, *C. fusiformis*, and *N. shiloi* are from floridoside and floridoside-related compounds. Relative high amounts of galactose residues (21–41 % of constituent monosaccharides) were already reported in the low molecular weight fraction of a hot water extract obtained from natural phytoplankton population dominated by *Skeletonema costatum* and species of *Heterosigma* (Raphidophyceae) [66]. Also, galactose residues were observed in variable amounts in a warm water extract of different diatoms, including in *C. fusiformis* (11 mol%) [62]. Although in both studies, the occurrence of floridoside and/or isofloridoside in the diatoms has been hypothesised, these compounds have not been identified or quantified. In addition, when subjected to high salinity conditions, diatom species *Phaeodactylum tricornutum, Thalassiosira pseudonana*, and *Skeletonema marinoi* produced a putatively identified glyceryl-glycoside, along with other metabolites possibly related with a diatom osmoadaptation [67]. Floridoside is a photosynthetic product that acts as an osmoregulator, important for cell protection under hypersaline conditions [65]. Different biological activities have been attributed to floridoside, such as immunoregulatory [68], antioxidant [69], anti-inflammatory [70], anti-bacterial and antifouling properties [71].

The source of ribose in the three diatom species is still unclear. Previous studies have attributed the ribose detected in diatoms to intracellular RNA or nucleotides and co-factors [62,72,73]. The remaining monosaccharides residues quantified, namely uronic acids, mannose, xylose, fucose, rhamnose, glucosamine, and the naturally methylated sugars could correspond to cell wall polysaccharides, also called frustule, or to extracellular polysaccharides (EPS) that are still bounded to the cell wall. The cell wall monosaccharide residues of multiple diatoms are composed of high amounts of mannose and glucuronic acid and low amounts of fucose and xylose [74]. The EPS excreted by diatoms are heterogenous polysaccharides that greatly differ in monosaccharide residues, sulfate content, and glycosidic linkages among different growth conditions and diatom species [74]. The GlcN identified could be due to the presence of chitin. Chitin has been described as being part of the *Thalassiosira pseudonana* cell wall [75], and it was hypothesised that chitin could be commonly underestimated as a component of diatom cells [74].

In terms of potential health-promoting benefits and applications, it is important to highlight that diatom *N. shiloi* revealed the highest content of chrysolaminaran, with potential immunostimulatory activity, as reported for these insoluble glucans [76], and floridoside, also associated to bioactive properties.

3.6. Amino acids composition and peptide profile

The amino acid profile of the three microalgae species (Fig. 5) revealed variations in the quantity of the amino acids produced. The total content of amino acids ranged from 27 g 100 g DW biomass^{-1} in *C. fusiformis*, 35 g 100 g^{-1} DW in *N. shiloi*, and 44 g 100 g^{-1} DW in *C. calcitrans*.

C. calcitrans consistently showed the highest levels of several amino acids, particularly aspartic acid, glutamic acid, alanine, and leucine. The high concentration of these amino acids suggested that *C. calcitrans* might have a more active protein synthesis or greater capacity for producing amino acids and overall nutritional value than the other species under study. The most abundant amino acids also align with the amino acid profile previously reported for *C. calcitrans* [77].

The essential amino acids content in the diatoms – *C. calcitrans* (36 %), *C. fusiformis* (35 %), and *N. shiloi* (36 %) – indicate a considerable proportion of essential amino acids relative to their total amino acid content, which has important implications for their nutritional value. Each species contains >35 % essential amino acids, which are vital because the human body cannot synthesise them and must be obtained through diet [78]. Therefore, with their high essential amino acid content, these microalgae species have strong potential as sustainable, high-quality sources of essential amino acids. This rich profile makes them ideal candidates for use in functional ingredients, protein supplements, and as additives to enhance the amino acid profile of various food and feed products. Such applications hold promise for both health-focused foods and industrial developments aimed at creating nutritionally enhanced products, making these microalgae valuable for supporting balanced diets and addressing essential amino acid needs [79].

Although the protein content of the diatoms studied varies significantly, the nutritional profiles regarding amino acid composition remain notably similar. While *C. calcitrans* exhibited the highest protein content (30.14 %), its amino acid profile, particularly the balance of essential and non-essential amino acids, aligns closely with the other species. This finding underscores the importance of evaluating the total protein content and the specific amino acid compositions to fully assess the nutritional value of these microalgae. For instance, all three species demonstrated comparable proportions of essential amino acids (approximately 35–36 %), a critical factor for their use in dietary applications.

The highest content of amino acids found for *C. calcitrans* is in line with its highest protein content determined by elemental analysis (Table 1), as well as the chromatographic profiles obtained by size exclusion chromatography (SEC) with detection at 280 nm (Supplementary Fig. S13). The chromatograms revealed distinct patterns in soluble protein/peptide size distribution among the diatom species, reflected by variations in absorbance peaks across different molecular weight ranges (>50 kDa, 10–50 kDa, 5–10 kDa, 3–5 kDa, 1–3 kDa, and < 1 kDa). *C. calcitrans* consistently exhibited the highest absorbance across all molecular weight ranges, mainly at the highest molecular weight region (>50 kDa), which is indicative of the presence of large

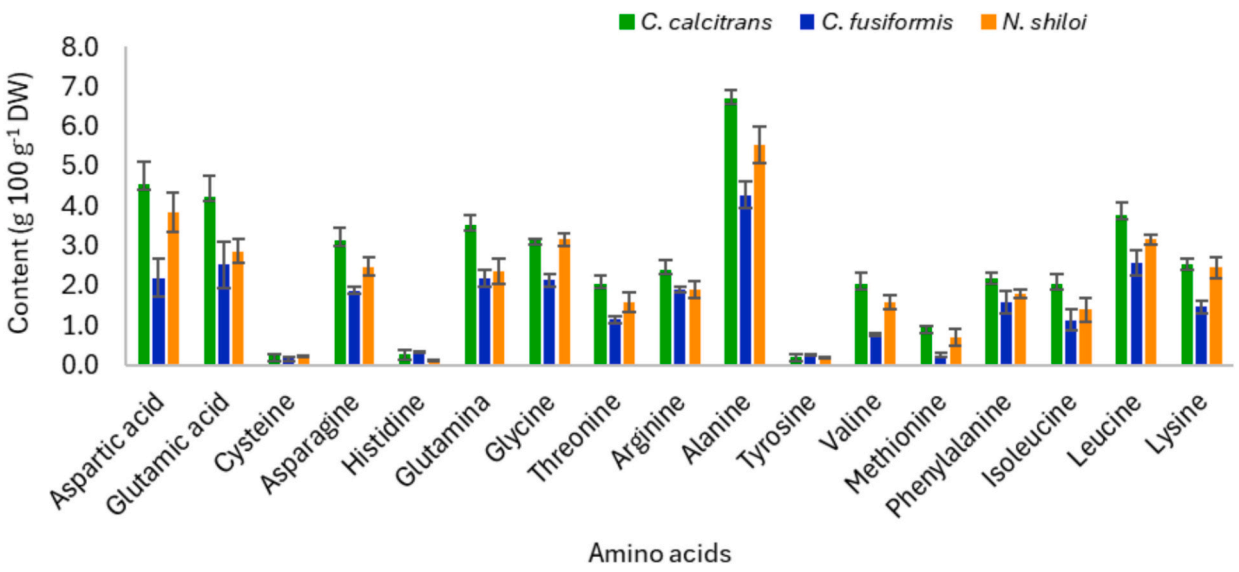

Fig. 5. Amino acids content (g 100 g^{-1} DW) of *C. calcitrans*, *C. fusiformis*, and *N. shiloi* diatoms. The graph shows the content of various amino acids, including both essential (threonine, valine, methionine, phenylalanine, isoleucine, leucine, and lysine) and non-essential (aspartic acid, glutamic acid, cysteine, asparagine, glutamine, glycine, arginine, alanine, and tyrosine) types. Data are presented as mean ± standard deviation (SD) ($n = 3$).

protein complexes and at the lower molecular weight regions (1–3 kDa and < 1 kDa), indicative of the presence of peptides. Considering that bioactive peptides are often within these lower molecular weight fractions [79], these data suggest that *C. calcitrans* may be a valuable source of peptides. Microalgae-derived bioactive peptides have garnered significant interest as functional ingredients, namely antioxidant and antihypertensive compounds, known to promote cardiovascular health [80].

In summary, the superior amino acid content and protein and peptide diversity of *C. calcitrans* reinforce this diatom as a leading candidate for applications where both high protein content and a wide variety of peptides are desired.

3.7. Mineral profile

The mineral profile was also evaluated, with the results presented in Fig. 6. The minerals analysed included molybdenum (Mo), zinc (Zn), cadmium (Cd), lead (Pb), nickel (Ni), cobalt (Co), boron (B), manganese (Mn), iron (Fe), copper (Cu), aluminium (Al), phosphorus (P), magnesium (Mg), sodium (Na), potassium (K), calcium (Ca), selenium (Se) and chromium (Cr). Elements like Mo, Zn, Cd, Pb, Ni, Co, B, Mn, Cu, Se, and Cr were identified in trace amounts (< 0.18 mg.g DW biomass^{-1}) across all three species. Fe showed slightly higher levels compared to the other trace minerals, with *C. calcitrans* exhibiting the highest concentration (2.04 mg.g DW biomass^{-1}). The most predominant minerals in terms of concentration across the three diatom species were P, Mg, Na, K, and Ca. All three species showed similar levels of P, indicating a uniform uptake of this essential nutrient. K also exhibited relatively uniform levels across the algae. *C. calcitrans* contained the highest concentration of Na (32.01 mg.g^{-1} DW biomass), while the other two species exhibited lower and comparable values. However, the highest difference was observed in the Ca content, with 67.50 mg.g^{-1} found in *N. shiloi*, 26.61 mg.g^{-1} in *C. fusiformis* and 4.02 mg.g^{-1} in *C. calcitrans*.

The mineral profiles of these diatoms revealed considerable nutritional potential, primarily due to their high levels of essential macro minerals, such as P, Mg, Na, K, and Ca. For instance, P is vital for cellular

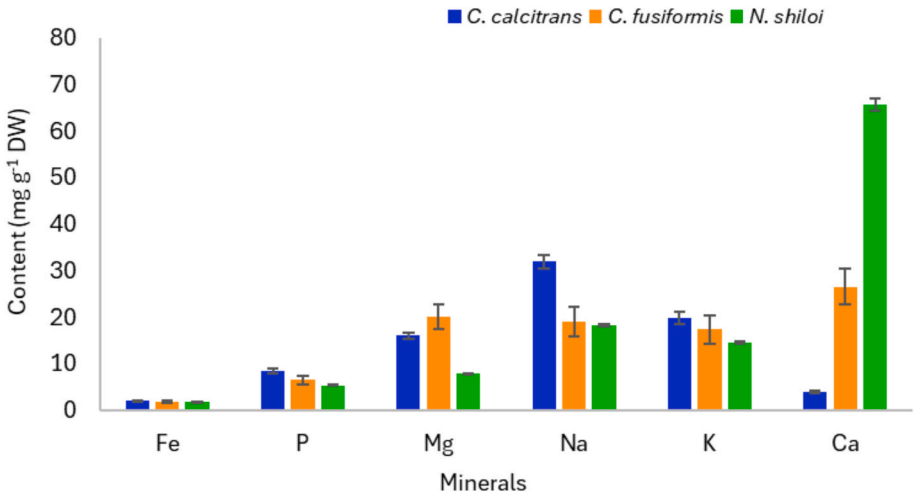

Fig. 6. Mineral content (mg g DW^{-1}) profiles of *N. shiloi*, *C. fusiformis*, and *C. calcitrans* diatoms. Abbreviations: Iron: Fe, Phosphorus: P, Magnesium: Mg, Sodium: Na, Potassium: K, Calcium: Ca. Elements detected in low concentrations (< 0.18 mg g DW biomass^{-1}), including Mo, Zn, Cd, Pb, Ni, Co, B, Mn, Cu, Se, and Cr, are not represented.

energy transfer [81], Mg supports muscle and nerve function [82,83], and K aids in heart health and blood pressure regulation [84]. The high concentration of Ca in *N. shiloi* makes it beneficial for bone health [85].

Overall, the data suggests that each specie's balanced mineral composition and specific strengths (e.g., high Ca concentration in *N. shiloi*) make these diatoms promising candidates for targeted nutritional applications. They could be used in functional foods, dietary supplements, or as mineral-rich additives in animal feed, meeting a range of nutritional requirements and promoting health benefits.

4. Conclusions

The results of this study demonstrated that the selected diatoms – *N. shiloi*, *C. fusiformis*, and *C. calcitrans* – possess distinct and valuable biochemical compositions for food and feed applications. Among these, *C. calcitrans* emerges as a promising candidate for added-value applications due to its highest protein content, diverse peptide profile, and elevated levels of *n*-3 polyunsaturated fatty acids (PUFA), particularly eicosapentaenoic acid (EPA), and also interesting polar lipids with bioactive potential or to be used as ingredients in different sectors. These make *C. calcitrans* especially suited for protein-rich applications and nutraceutical formulations. Additionally, its higher content of pigments (chlorophylls and carotenoids) reinforces its potential as a source of bioactive compounds beneficial for health. Among the species analysed, *N. shiloi* also showed the highest content of bioactive carbohydrates and derivatives, chrysolaminaran and floridoside. *N. shiloi* could also be considered a mineral supplement, particularly for populations suffering from Ca deficiencies.

The overall high-quality protein, bioactive lipids, and specific mineral compositions found in these diatoms present exciting opportunities for application beyond aquaculture, including in the nutraceutical, cosmeceutical or pharmaceutical sectors, as well as for human nutrition. The species-specific profiles of these diatoms highlight their versatile potential across various sectors related to health and nutrition of both humans and animals.

Supplementary data to this article can be found online at https://doi.org/10.1016/j.algal.2025.104080.

CRediT authorship contribution statement

Ana S.P. Moreira: Writing – review & editing, Writing – original draft, Validation, Methodology, Formal analysis, Conceptualization. **Helena R. Rocha:** Writing – review & editing, Methodology, Formal analysis. **Susana Aveiro:** Writing – review & editing, Methodology, Formal analysis. **Andreia S. Ferreira:** Methodology, Formal analysis, Conceptualization. **Kayane Oliveira:** Writing – review & editing, Methodology, Formal analysis. **Alexandra Conde:** Writing – review & editing, Methodology, Formal analysis. **Marta Coelho:** Writing – review & editing, Validation, Methodology, Formal analysis. **Alexandre M.C. Rodrigues:** Writing – review & editing, Resources, Conceptualization. **Natacha Coelho:** Writing – review & editing, Resources, Conceptualization. **Hugo Pereira:** Writing – review & editing, Resources. **Ana Gomes:** Writing – review & editing, Conceptualization. **Manuela Pintado:** Writing – review & editing, Conceptualization. **Cláudia Nunes:** Writing – review & editing, Validation. **Manuel A. Coimbra:** Writing – review & editing, Conceptualization. **Sónia P.M. Ventura:** Writing – review & editing, Validation. **Rosário Domingues:** Writing – review & editing, Writing – original draft, Validation, Supervision, Project administration, Conceptualization. **Diana Lopes:** Writing – review & editing, Writing – original draft, Validation, Conceptualization.

Funding

This work was financially supported by "Pacto da Bioeconomia azul" (Project No. 16 with the application No. C644915664-00000026) within the WP5 Algae Vertical, funded by Next Generation EU European Fund and the Portuguese Recovery and Resilience Plan (PRR), under the scope of the incentive line "Agendas for Business Innovation" through the funding scheme C5 - Capitalization and Business Innovation.

Declaration of competing interest

The authors declare no conflict of interest.

Acknowledgments

The work was supported through the CESAM (UIDP/50017/2020 + UIDB/50017/2020 + LA/P/0094/2020), LAQV-REQUIMTE (UIDB/50006/2020 and UIDP/50006/2020) and CICECO-Aveiro Institute of Materials (UIDB/50011/2020 - DOI 10.54499/UIDB/50011/2020, UIDP/50011/2020 - DOI 10.54499/UIDP/50011/2020 & LA/P/0006/2020 - DOI 10.54499/LA/P/0006/2020), financed by national funds through the FCT/MCTES (PIDDAC).

Data availability

Data will be made available on request.

References

[1] R. Gordon, D. Losic, M.A. Tiffany, S.S. Nagy, F.A.S. Sterrenburg, The **g**lass **m**enagerie: diatoms for novel applications in nanotechnology, Trends Biotechnol. 27 (2009) 116–127.
[2] C.B. Field, M.J. Behrenfeld, J.T. Randerson, P. Falkowski, Primary production of the biosphere: integrating terrestrial and oceanic components, Science 281 (1998) 237–240.
[3] V. Smetacek, Diatoms and the ocean carbon cycle, Protist 150 (1999) 25–32.
[4] M.D. Kurkuri, C. Saunders, P.J. Collins, H. Pavic, D. Losic, Combining micro and nanoscale structures: emerging applications of diatoms, Micro and Nanosystems 3 (2011) 277–283.
[5] D.G. Mann, S.J.M. Droop, Biodiversity, biogeography and conservation of diatoms, in: J. Kristiansen (Ed.), Biogeography of Freshwater Algae: Proceedings of the Workshop on Biogeography of Freshwater Algae, **H**eld during the Fifth International Phycological Congress, Qingdao, China, June 1994, Springer Netherlands, Dordrecht, 1996, pp. 19–32.
[6] P. Jin, S. Agustí, Fast adaptation of tropical diatoms to increased warming with trade-offs, Sci. Rep. 8 (2018).
[7] Z. Yi, M. Xu, X. Di, S. Brynjolfsson, W. Fu, Exploring valuable lipids in diatoms, Front. Mar. Sci. 4 (2017).
[8] R. Dhanker, A. Saxena, A. Tiwari, P. Kumar Singh, A. Kumar Patel, H.U. Dahms, J. S. Hwang, G.M. González-Meza, E.M. Melchor-Martínez, H.M.N. Iqbal, et al., Towards sustainable diatom biorefinery: **r**ecent trends in cultivation and applications, Bioresour. Technol. 391 (2024) 3.
[9] L. Barra, R. Chandrasekaran, F. Corato, C. Brunet, The challenge of ecophysiological biodiversity for biotechnological applications of marine microalgae, Mar. Drugs 12 (2014) 1641–1675.
[10] W. Fu, K. Wichuk, S. Brynjólfsson, Developing diatoms for value-added products: **c**hallenges and opportunities, New Biotechnol. 32 (2015) 547–551.
[11] C. Vílchez, E. Forján, M. Cuaresma, F. Bédmar, I. Garbayo, J.M. Vega, Marine carotenoids: **b**iological functions and commercial applications, Mar. Drugs 9 (2011) 319–333.
[12] T. Lebeau, J.M. Robert, Diatom cultivation and biotechnologically relevant products. Part I: **c**ultivation at various scales, Appl. Microbiol. Biotechnol. 60 (2003) 612–623.
[13] P. Kuczynska, M. Jemiola-Rzeminska, K. Strzalka, Photosynthetic pigments in diatoms, Mar. Drugs 13 (2015) 5847–5881.
[14] T.T. Zhang, J. Xu, Y.M. Wang, C.H. Xue, Health benefits of dietary marine DHA/EPA-enriched glycerophospholipids, Prog. Lipid Res. 75 (2019) 20.
[15] L. Burri, N. Hoem, S. Banni, K. Berge, Marine omega-3 phospholipids: metabolism and biological activities, Int. J. Mol. Sci. 13 (2012) 15401–15419.
[16] P. Nieri, S. Carpi, R. Esposito, M. Costantini, V. Zupo, Bioactive molecules from marine diatoms and their value for the nutraceutical industry, Nutrients 15 (2023).
[17] F. Hentati, L. Tounsi, D. Djomdi, G. Pierre, C. Delattre, A.V. Ursu, I. Fendri, S. Abdelkafi, P. Michaud, Bioactive polysaccharides from seaweeds, Molecules 25 (2020).
[18] R. Alcázar, T. Altabella, F. Marco, C. Bortolotti, M. Reymond, C. Koncz, P. Carrasco, A.F. Tiburcio, Polyamines: **m**olecules with regulatory functions in plant abiotic stress tolerance, Planta 231 (2010) 1237–1249.
[19] S. Kopriva, A. Koprivova, Sulfate assimilation and glutathione synthesis in C4 plants, Photosynth. Res. 86 (2005) 363–372.
[20] D.V. Vavilin, W.F.J. Vermaas, Regulation of the tetrapyrrole biosynthetic pathway leading to heme and chlorophyll in plants and cyanobacteria, Physiol. Plant. 115 (2002) 9–24.
[21] M.R. Brown, S.W. Jeffrey, The amino acid and gross composition of marine diatoms potentially useful for mariculture, J. Appl. Phycol. 7 (1995) 521–527.

[22] S.M. Tibbetts, J.E. Milley, S.P. Lall, Chemical composition and nutritional properties of freshwater and marine microalgal biomass cultured in photobioreactors, J. Appl. Phycol. 27 (2015) 1109–1119.

[23] I. Barkia, L. Al-Haj, A. Abdul Hamid, M. Zakaria, N. Saari, F. Zadjali, Indigenous marine diatoms as novel sources of bioactive peptides with antihypertensive and antioxidant properties, Int. J. Food Sci. Technol. 54 (2019) 1514–1522.

[24] M.A.J. Alzahrani, C.O. Perera, Y. Hemar, Production of bioactive proteins and peptides from the diatom *Nitzschia laevis* and comparison of their *in vitro* antioxidant activities with those from *Spirulina platensis* and *Chlorella vulgaris*, Int. J. Food Sci. Technol. 53 (2018) 676–682.

[25] V. Margaras, M. Pape, F. Scholaert, A.B. Wilson, The blue economy: Overview and EU policy framework, Availabe online: **https://policycommons.net/artifacts/1337377/the-blue-economy/1945205/** (accessed on 6th January 2025.

[26] A.S.P. Moreira, J. Gonçalves, T.A. Conde, D. Couto, T. Melo, I.B. Maia, H. Pereira, J. Silva, M.R. Domingues, C. Nunes, *Chrysotila pseudoroscoffensis* as a source of high-value polar lipids with antioxidant activity: **a** lipidomic approach, Algal Res. 66 (2022) 102756.

[27] S.O. Lourenço, E. Barbarino, P.L. Lavín, U.M. Lanfer Marquez, E. Aidar, Distribution of intracellular nitrogen in marine microalgae: **c**alculation of new nitrogen-to-protein conversion factors, Eur. J. Phycol. 39 (2004) 17–32.

[28] M. Grubišić, B. Šantek, Z. Zorić, Z. Čošić, I. Vrana, B. Gašparović, R. Čož-Rakovac, M. Ivančić Šantek, Bioprospecting of microalgae isolated from the Adriatic **S**ea: characterization of biomass, pigment, lipid and fatty acid composition, and antioxidant and antimicrobial activity, Molecules 27 (2022) 1248.

[29] B.M.C. Vaz, M. Martins, L.M. de Souza Mesquita, M.C. Neves, A.P.M. Fernandes, D. C.G.A. Pinto, M.G.P.M.S. Neves, J.A.P. Coutinho, S.P.M. Ventura, Using aqueous solutions of ionic liquids as chlorophyll eluents in solid-phase extraction processes, Chem. Eng. J. 428 (2022) 131073.

[30] J. Folch, M. Lees, G.H. Sloane Stanley, A simple method for the isolation and purification of total lipides from animal tissues, J. Biol. Chem. 226 (1957) 497–509.

[31] A.S. Ferreira, S.S. Ferreira, A. Correia, M. Vilanova, T.H. Silva, M.A. Coimbra, C. Nunes, Reserve, structural and extracellular polysaccharides of *Chlorella vulgaris*: **a** holistic approach, Algal Res. 45 (2020) 101757.

[32] G.R. Lopes, A.S. Ferreira, M. Pinto, C.P. Passos, E. Coelho, C. Rodrigues, C. Figueira, S.M. Rocha, F.M. Nunes, M.A. Coimbra, Carbohydrate content, dietary fibre and melanoidins: **c**omposition of espresso from single-dose coffee capsules, Food Res. Int. 89 (2016) 989–996.

[33] R. Gómez-García, D.A. Campos, C.N. Aguilar, A.R. Madureira, M. Pintado, Biological protein precipitation: **a** green process for the extraction of cucumisin from melon (*Cucumis melo* L. *inodorus*) by-products, Food Hydrocoll. 116 (2021) 106650.

[34] MARS 6 - Microwave Acid Digestion, In *Method Note Compendium* (2019) 23.

[35] M. Hildebrand, S.J.L. Lerch, R.P. Shrestha, Understanding diatom cell wall silicification - moving forward, Front. Mar. Sci. 5 (2018).

[36] F. Mus, J.-P. Toussaint, K.E. Cooksey, M.W. Fields, R. Gerlach, B.M. Peyton, R. P. Carlson, Physiological and molecular analysis of carbon source supplementation and pH stress-induced lipid accumulation in the marine diatom *Phaeodactylum tricornutum*, Appl. Microbiol. Biotechnol. 97 (2013) 3625–3642.

[37] H. Abida, L.-J. Dolch, C. Meï, V. Villanova, M. Conte, M.A. Block, G. Finazzi, O. Bastien, L. Tirichine, C. Bowler, et al., Membrane glycerolipid remodeling triggered by nitrogen and phosphorus starvation in *Phaeodactylum tricornutum*, Plant Physiol. 167 (2014) 118–136.

[38] N. Yodsuwan, S. Sawayama, S. Sirisansaneeyakul, Effect of nitrogen concentration on growth, lipid production and fatty acid profiles of the marine diatom *Phaeodactylum tricornutum*, **a**griculture and **n**atural, Resources 51 (2017) 190–197.

[39] C.R.V. Bastos, I.B. Maia, H. Pereira, J. Navalho, J.C.S. Varela, Optimisation of biomass production and nutritional value of two marine diatoms (Bacillariophyceae), *Skeletonema costatum* and *Chaetoceros calcitrans*, Biology 11 (2022).

[40] J.I. Carreto, J.A. Catoggio, Variations in pigment contents of the diatom *Phaeodactylum tricornutum* during growth, Mar. Biol. 36 (1976) 105–112.

[41] S.C. Foo, F.M. Yusoff, M.U. Imam, J.B. Foo, N. Ismail, N.H. Azmi, Y.S. Tor, N.M. H. Khong, M. Ismail, Increased fucoxanthin in *Chaetoceros calcitrans* extract exacerbates apoptosis in liver cancer cells via multiple targeted cellular pathways, Biotechnology Reports 21 (2019).

[42] A. Sharma, P. Singh, P. Srivastava, Photosynthetic pigments in diatoms, in: P. Srivastava, A.S. Khan, J. Verma, S. Dhyani (Eds.), Insights into the World of Diatoms: From Essentials to Applications, Springer Nature Singapore, Singapore, 2023, pp. 1–20.

[43] G.E. Napolitano, R.G. Ackman, W.M.N. Ratnayake, Fatty acid composition of three cultured algal species (*Isochvysis galbana*, *Chaetoceros gracilis* and *Chaetoceros calcitrans*) used as food for bivalve larvae, J. World Aquacult. Soc. 21 (1990) 122–130.

[44] R.G. Gevorgiz, A.A. Gontcharov, S.N. Zheleznova, L.V. Malakhova, T.E. Alyomova, T. Maoka, M.V. Nekhoroshev, Biotechnological potential of a new strain of *Cylindrotheca fusiformis* producing fatty acids and fucoxanthin, Bioresource Technology Reports 18 (2022) 101098.

[45] M. Brett, D. Müller-Navarra, The role of highly unsaturated fatty acids in aquatic foodweb processes, Freshw. Biol. 38 (1997) 483–499.

[46] Nomenclature in MS-DIAL lipidomics, Availabe online: **https://systemsomicslab.github.io/compms/msdial/lipidnomenclature.html**. accessed on 6th January 2025.

[47] M.J. Conroy, R.M. Andrews, S. Andrews, L. Cockayne, E.A. Dennis, E. Fahy, C. Gaud, W.J. Griffiths, G. Jukes, M. Kolchin, et al., LIPID MAPS: update to databases and tools for the lipidomics community, Availabe online: **https://www.lipidmaps.org/**. accessed on 6th January 2025.

[48] R. Anderson, B.P. Livermore, B.E. Volcani, M. Kates, A novel sulfonolipid in diatoms, Biochim. Biophys. Acta 409 (1975) 259–263.

[49] C.D. Radka, D.J. Miller, M.W. Frank, C.O. Rock, Biochemical characterization of the first step in sulfonolipid biosynthesis in *Alistipes finegoldii*, J. Biol. Chem. 298 (2022) 25.

[50] J. Jouhet, E. Alves, Y. Boutté, S. Darnet, F. Domergue, T. Durand, P. Fischer, L. Fouillen, M. Grube, J. Joubès, et al., Plant and algal lipidomes: **a**nalysis, composition, and their societal significance, Prog. Lipid Res. 96 (2024) 31.

[51] J. Holmbäck, A.A. Karlsson, K.C. Arnoldsson, Characterization of N-acylphosphatidylethanolamine and acylphosphatidylglycerol in oats, Lipids 36 (2001) 153–165.

[52] J. Matos, C. Cardoso, A. Gomes, A.M. Campos, P. Falé, C. Afonso, N.M. Bandarra, Bioprospection of Isochrysis galbana and its potential as a nutraceutical, Food Funct. 10 (2019) 7333–7342.

[53] E.T. Lain, N. Agrawal, E. Ruvolo, J.M. Weise, V.D. Callender, The role of coenzyme Q10 in skin aging and opportunities for topical intervention: a review, J. Clin. Aesthet. Dermatol. 17 (2024) 50–55.

[54] D. Couto, T.A. Conde, T. Melo, B. Neves, M. Costa, J. Silva, R. Domingues, P. Domingues, The chemodiversity of polar lipidomes of microalgae from different taxa, Algal Res. 70 (2023) 103006.

[55] S. Wang, D. Sirbu, L. Thomsen, N. Kuhnert, M.S. Ullrich, C. Thomsen, Comparative lipidomic studies of *Scenedesmus* sp. (Chlorophyceae) and *Cylindrotheca closterium* (Bacillariophyceae) reveal their differences in lipid production under nitrogen starvation, J. Phycol. 55 (2019) 1246–1257.

[56] S.S. Aveiro, T. Melo, A. Figueiredo, P. Domingues, H. Pereira, I.B. Maia, J. Silva, M. R. Domingues, C. Nunes, A.S.P. Moreira, The polar lipidome of cultured *Emiliania huxleyi*: **a** source of bioactive lipids with relevance for biotechnological applications, Biomolecules 10 (2020) 1434.

[57] T. Conde, D. Lopes, W. Łuczaj, B. Neves, B. Pinto, T. Maurício, P. Domingues, E. Skrzydlewska, M.R. Domingues, Algal lipids as modulators of skin disease: a critical review, Metabolites 12 (2022).

[58] M.E. Leser, L. Sagalowicz, M. Michel, H.J. Watzke, Self-assembly of polar food lipids, Adv. Colloid Interf. Sci. 123-126 (2006) 125–136.

[59] C. Robert, A. Penhoat, L. Couëdelo, M. Monnoye, D. Rainteau, E. Meugnier, S. Bary, H. Abrous, E. Loizon, P. Krasniqi, et al., Natural emulsifiers lecithins preserve gut microbiota diversity in relation with specific faecal lipids in high fat-fed mice, J. Funct. Foods 105 (2023) 105540.

[60] S. Kalepu, M. Manthina, V. Padavala, Oral lipid-based drug delivery systems – an overview, Acta Pharm. Sin. B 3 (2013) 361–372.

[61] M. Traversier, T. Gaslondes, S. Milesi, S. Michel, E. Delannay, Polar lipids in cosmetics: recent trends in extraction, separation, analysis and main applications, Phytochem. Rev. 17 (2018) 1179–1210.

[62] A. Chiovitti, P. Molino, S.A. Crawford, R. Teng, T. Spurck, R. Wetherbee, The glucans extracted with warm water from diatoms are mainly derived from intracellular chrysolaminaran and not extracellular polysaccharides, Eur. J. Phycol. 39 (2004) 117–128.

[63] K.I. Reitan, G. Øie, H. Jørgensen, X. Wang, Chemical composition of selected marine microalgae, with emphasis on lipid and carbohydrate production for potential use as feed resources, J. Appl. Phycol. 33 (2021) 3831–3842.

[64] E. Granum, S.M. Myklestad, Effects of NH_4^+ assimilation on dark carbon fixation and β-1,3-glucan metabolism in the marine diatom *Skeletonema costatum* (Bacillariophyceae), J. Phycol. 35 (1999) 1191–1199.

[65] Z. Weng, J. Zhao, Z. Wang, J. Chen, Q. Luo, R. Yang, H. Chen, P. Zhang, T. Wang, Responses of isomeric floridosides under stress in two heteromorphic generations of *Neoporphyra haitanensis*, Algal Res. 65 (2022) 102724.

[66] J. Hama, N. Handa, Diel variation of water-extractable carbohydrate composition of natural phytoplankton populations in Kinu-**U**ra Bay, J. Exp. Mar. Biol. Ecol. 162 (1992) 159–176.

[67] V. Nikitashina, D. Stettin, G. Pohnert, Metabolic adaptation of diatoms to hypersalinity, Phytochemistry 201 (2022) 4.

[68] A. Courtois, C. Simon-Colin, C. Boisset, C. Berthou, E. Deslandes, J. Guézennec, A. Bordron, Floridoside extracted from the red alga *Mastocarpus stellatus* is a potent activator of the classical complement pathway, Mar. Drugs 6 (2008) 407–417.

[69] T. Niu, G. Fu, J. Zhou, H. Han, J. Chen, W. Wu, H. Chen, Floridoside exhibits antioxidant properties by activating HO-1 expression via p38/ERK MAPK pathway, Mar. Drugs 18 (2020) 105.

[70] M. Kim, Y.X. Li, P. Dewapriya, B. Ryu, S.K. Kim, Floridoside suppresses pro-inflammatory responses by blocking MAPK signaling in activated microglia, BMB Rep. 46 (2013) 398–403.

[71] H.B. Liu, K.P. Koh, J.S. Kim, Y. Seo, S. Park, The effects of betonicine, floridoside, and isethionic acid from the red alga *Ahnfeltiopsis flabelliformis* on quorum-sensing activity, Biotechnol, Bioprocess Eng. 13 (2008) 458–463.

[72] A. Chiovitti, M.J. Higgins, R.E. Harper, R. Wetherbee, A. Bacic, The complex polysaccharides of the raphid diatom *Pinnularia viridis* (Bacillariophyceae), J. Phycol. 39 (2003) 543–554.

[73] A. Haug, S. Myklestad, Polysaccharides of marine diatoms with special reference to *Chaetoceros* species, Mar. Biol. 34 (1976) 217–222.

[74] B. Gügi, T. Le Costaouec, C. Burel, P. Lerouge, W. Helbert, M. Bardor, Diatom-**s**pecific **o**ligosaccharide and **p**olysaccharide **s**tructures **h**elp to **u**nravel **b**iosynthetic **c**apabilities in **d**iatoms, Mar. Drugs 13 (2015) 5993–6018.

[75] B. Tesson, S. Masse, G. Laurent, J. Maquet, J. Livage, V. Martin-Jézéquel, T. Coradin, Contribution of multi-nuclear solid state NMR to the characterization of the *Thalassiosira pseudonana* diatom cell wall, Anal. Bioanal. Chem. 390 (2008) 1889–1898.

[76] R. Bastos, P.G. Oliveira, V.M. Gaspar, J.F. Mano, M.A. Coimbra, E. Coelho, Brewer's yeast polysaccharides - **a** review of their exquisite structural features and biomedical applications, Carbohydr. Polym. 277 (2022) 28.
[77] M.R. Brown, The amino-acid and sugar composition of 16 species of microalgae used in mariculture, J. Exp. Mar. Biol. Ecol. 145 (1991) 79–99.
[78] D.D. Church, K.R. Hirsch, S. Park, I.Y. Kim, J.A. Gwin, S.M. Pasiakos, R.R. Wolfe, A. A. Ferrando, Essential amino acids and protein synthesis: insights into maximizing the muscle and whole-body response to feeding, Nutrients 12 (2020).
[79] O.K. Mosibo, G. Ferrentino, C.C. Udenigwe, Microalgae proteins as sustainable ingredients in novel foods: recent developments and challenges, Foods 13 (2024) 733.
[80] C.E.C.C. Ejike, S.A. Collins, N. Balasuriya, A.K. Swanson, B. Mason, C.C. Udenigwe, Prospects of microalgae proteins in producing peptide-based functional foods for promoting cardiovascular health, Trends Food Sci. Technol. 59 (2017) 30–36.
[81] J.W.F. Nicholls, J.P. Chin, T.A. Williams, T.M. Lenton, V. O'Flaherty, J. W. McGrath, On the potential roles of phosphorus in the early evolution of energy metabolism, Front. Microbiol. 14 (2023).
[82] A.C.R. Souza, A.R. Vasconcelos, D.D. Dias, G. Komoni, J.J. Name, The integral role of magnesium in muscle integrity and aging: a comprehensive review, Nutrients 15 (2023) 5127.
[83] A.E. Kirkland, G.L. Sarlo, K.F. Holton, The role of magnesium in neurological disorders, Nutrients 10 (2018).
[84] R.J. Chan, N. Parikh, S. Ahmed, M. Ruzicka, S. Hiremath, Blood pressure control should focus on more potassium: controversies in hypertension, Hypertension 81 (2024) 501–509.
[85] L. Vannucci, C. Fossi, S. Quattrini, L. Guasti, B. Pampaloni, G. Gronchi, F. Giusti, C. Romagnoli, L. Cianferotti, G. Marcucci, et al., Calcium intake in bone health: a focus on calcium-rich mineral waters, Nutrients 10 (2018).